



Photon Reconstruction and Performance at ATLAS and CMS

Seth Zenz

On behalf of the ATLAS and CMS Collaborations

PPSHC2015 - LPNHE - Paris, France

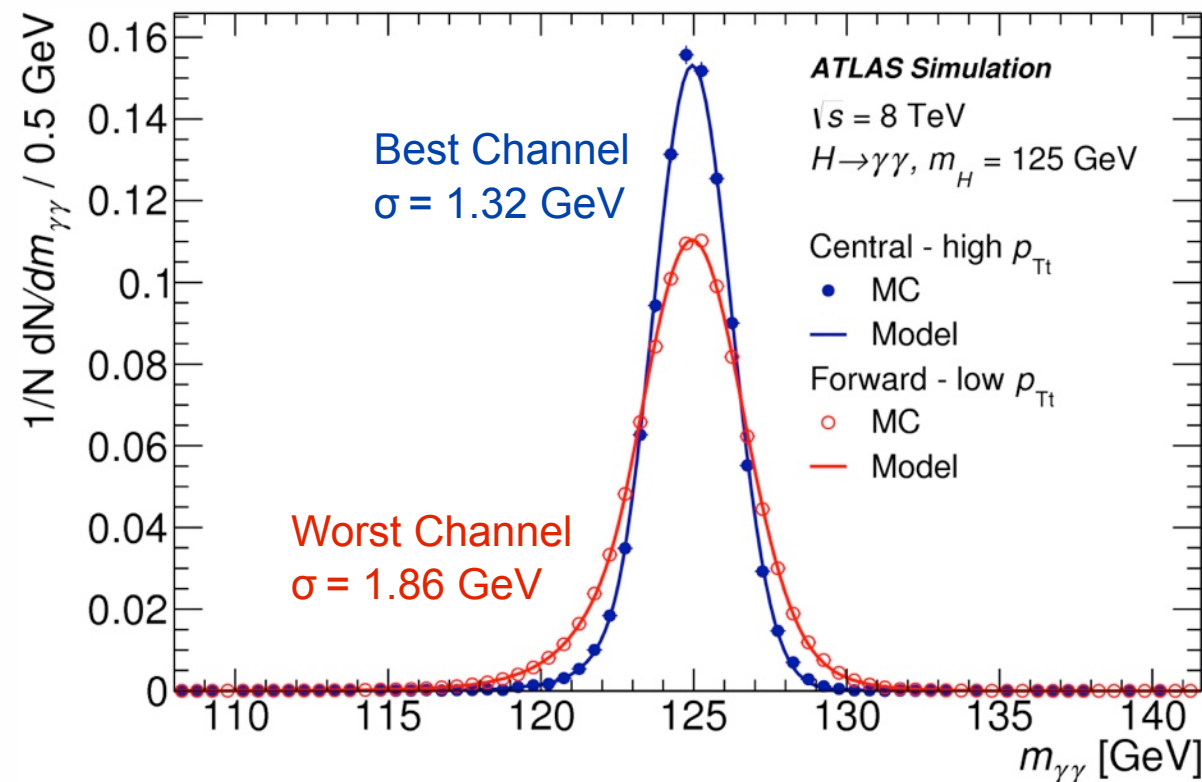
18 May 2015



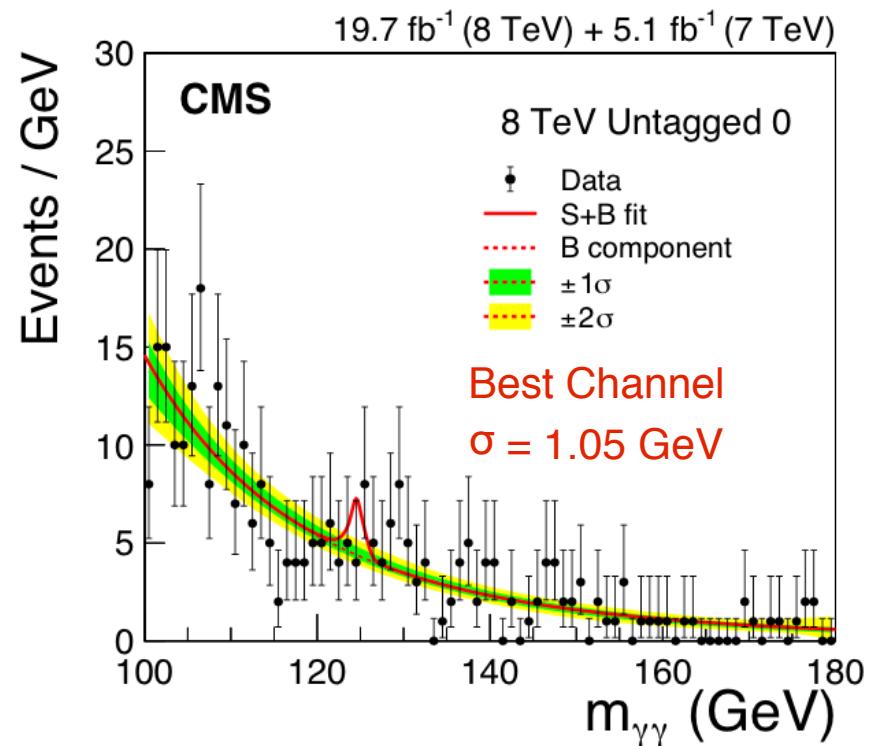
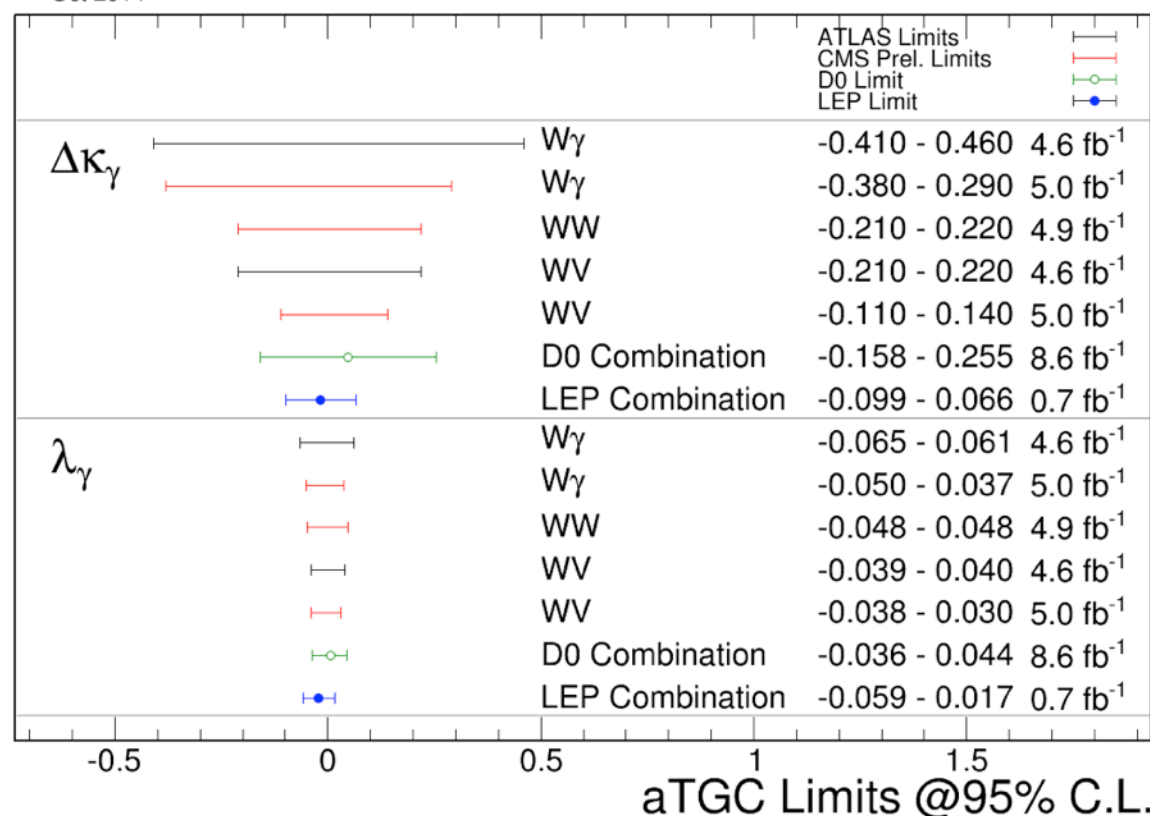
- Physics motivation
- LHC, ATLAS, and CMS
- Electromagnetic calorimeters: layout and calibration
- Photon reconstruction
 - Window algorithms
 - Conversion reconstruction
 - Pointing and vertexing
- Energy
 - Regression MVA
 - Scale, cross-checks, material
- Final identification / selection
- Looking toward Run 2

- Photon reconstruction is key to Standard Model measurements and new physics searches
- Energy and angular resolution both critical: $m_{\gamma\gamma}^2 = 2E_1E_2(1 - \cos\Delta\alpha)$
- ATLAS and CMS approaches differ, but both have excellent results

Phys. Rev. D 90, 112015 (2014)



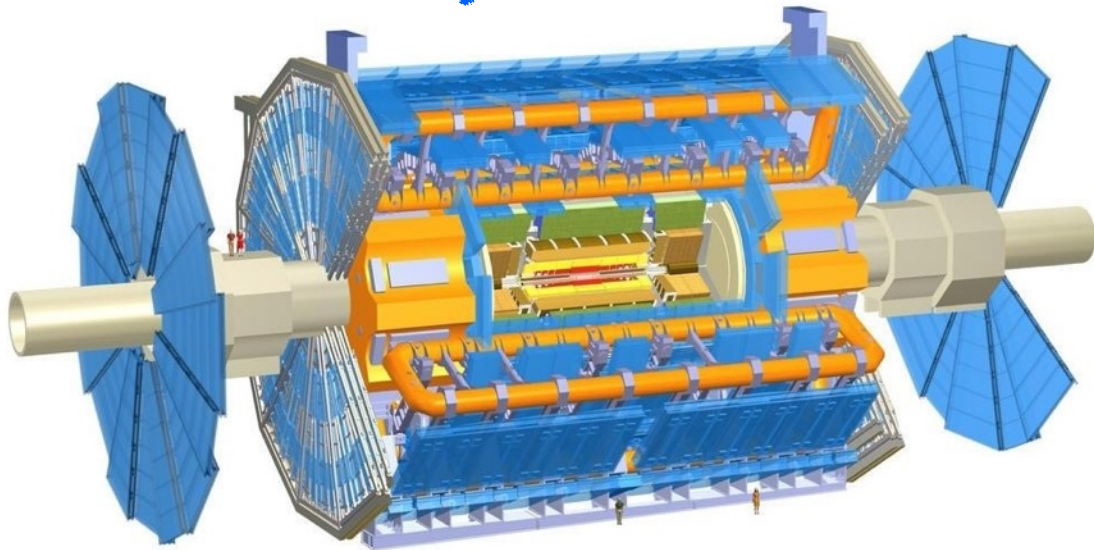
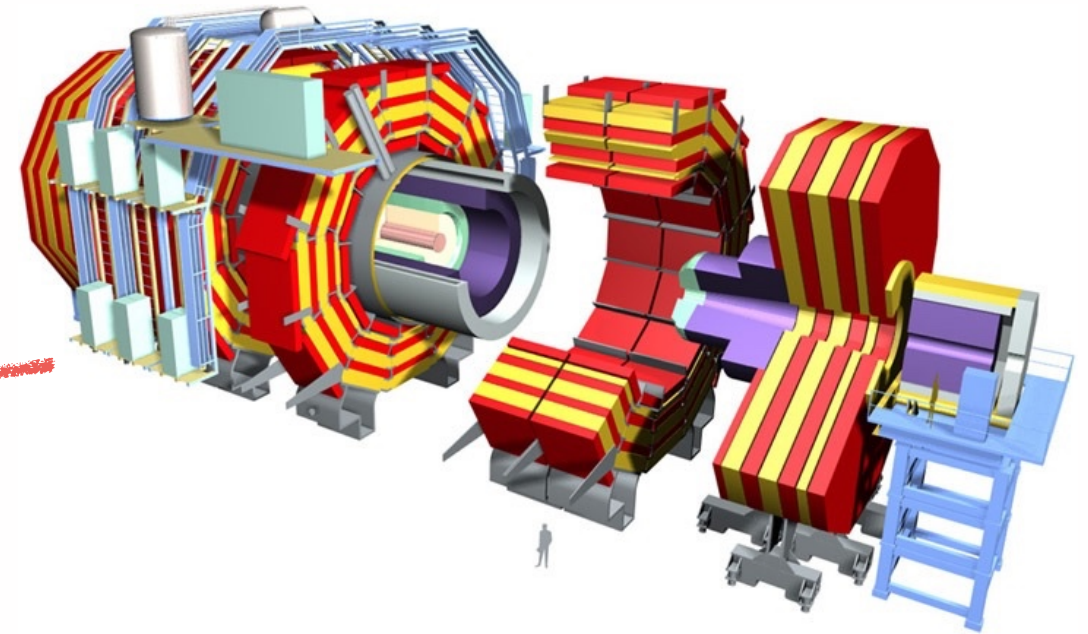
Oct 2014



Worst Channel
 $\sigma = 2.62 \text{ GeV}$

CMS-HIG-13-001

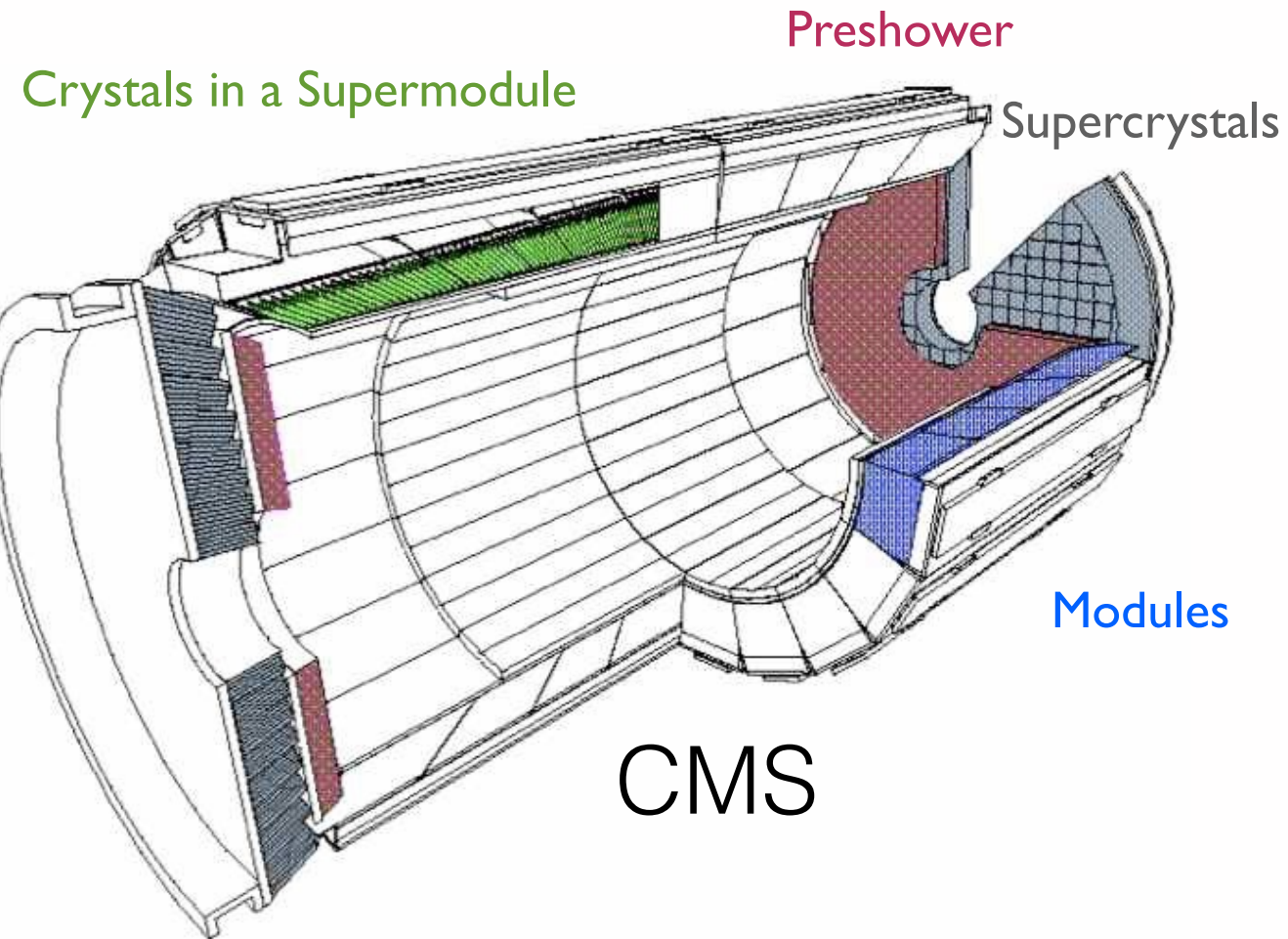
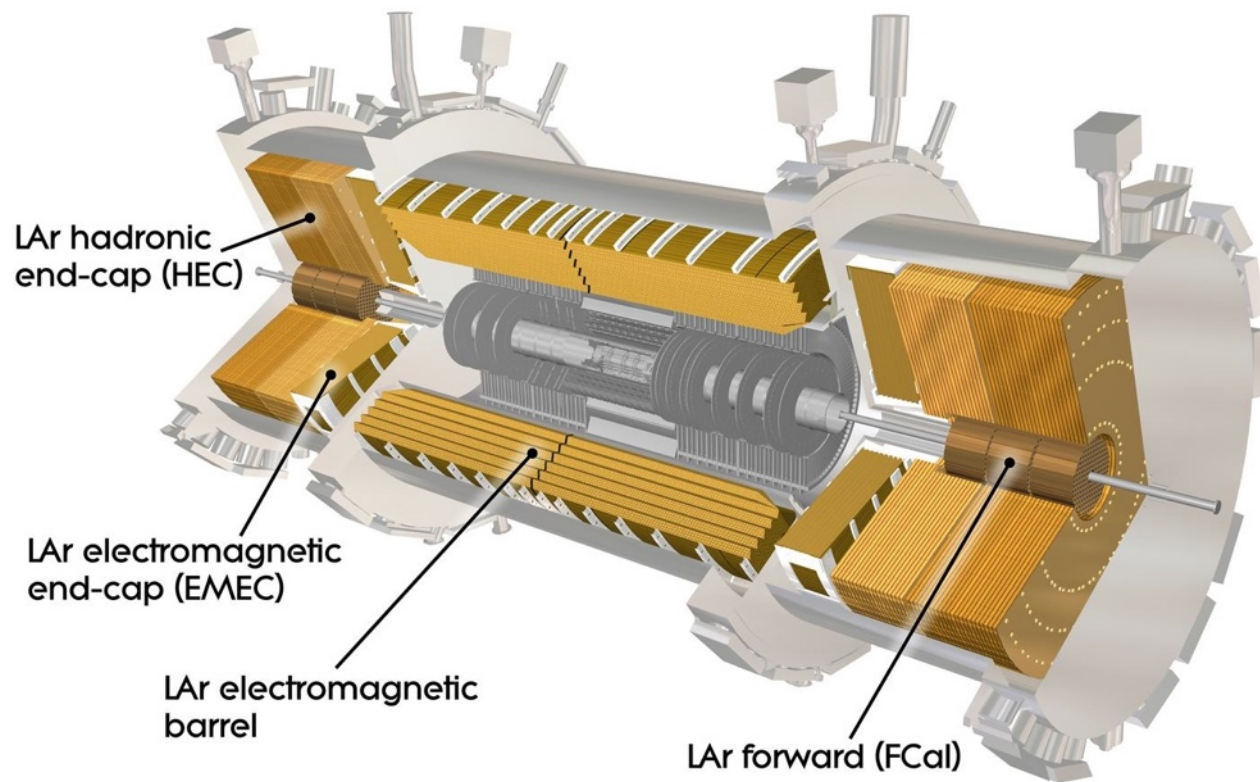
Sources/details: <https://twiki.cern.ch/twiki/bin/view/CMSPublic/PhysicsResultsSMPaTGC>

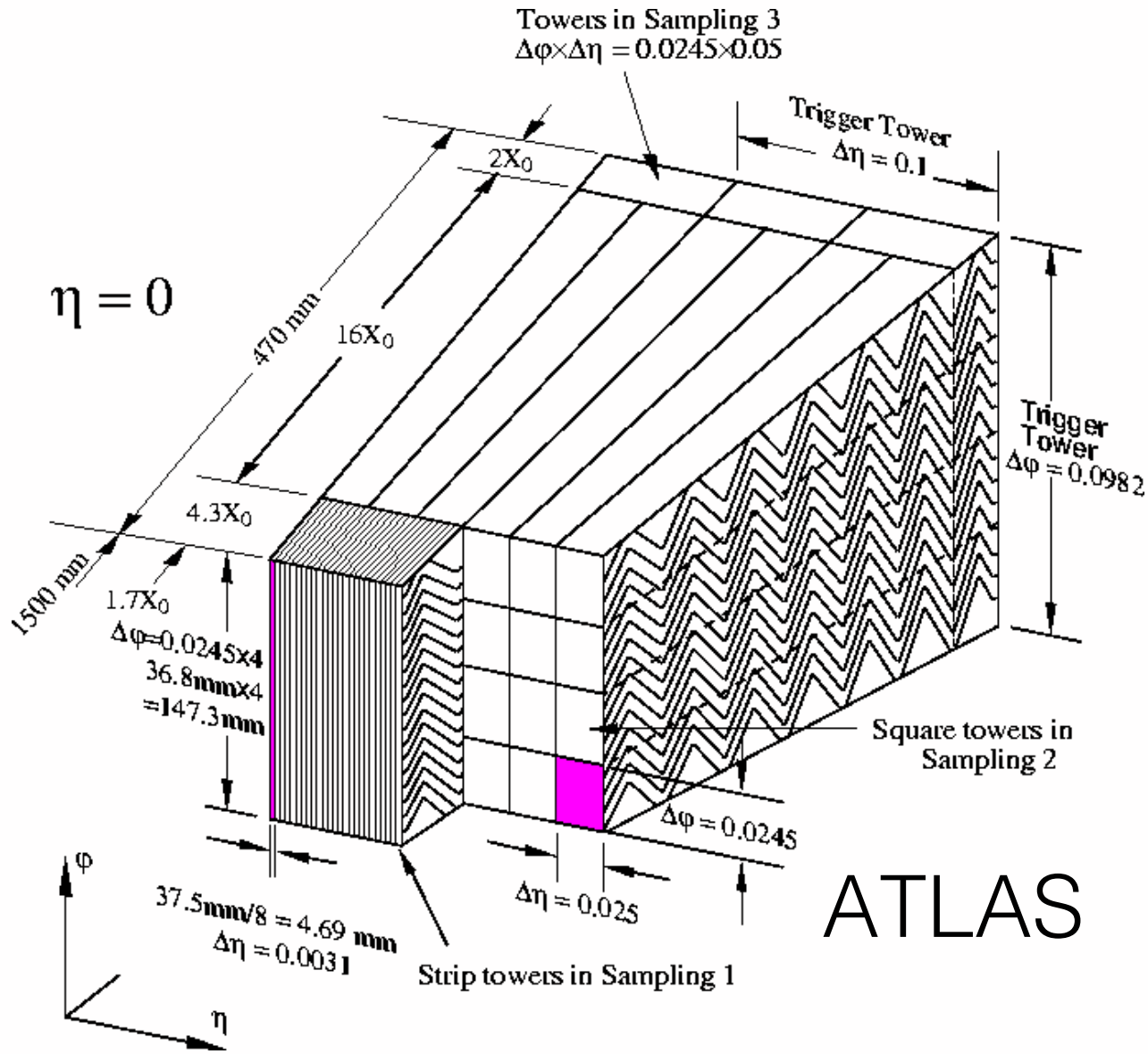


- LHC Run 1: 7-8 TeV, 50ns, ~20 PU
 - Run 2: 13 TeV, 25ns, ~40 PU
- CMS: 3.8 T solenoid, all-Si tracker
- ATLAS: 2T solenoid, 7 Si layers + Transition Radiation Tracker (TRT)

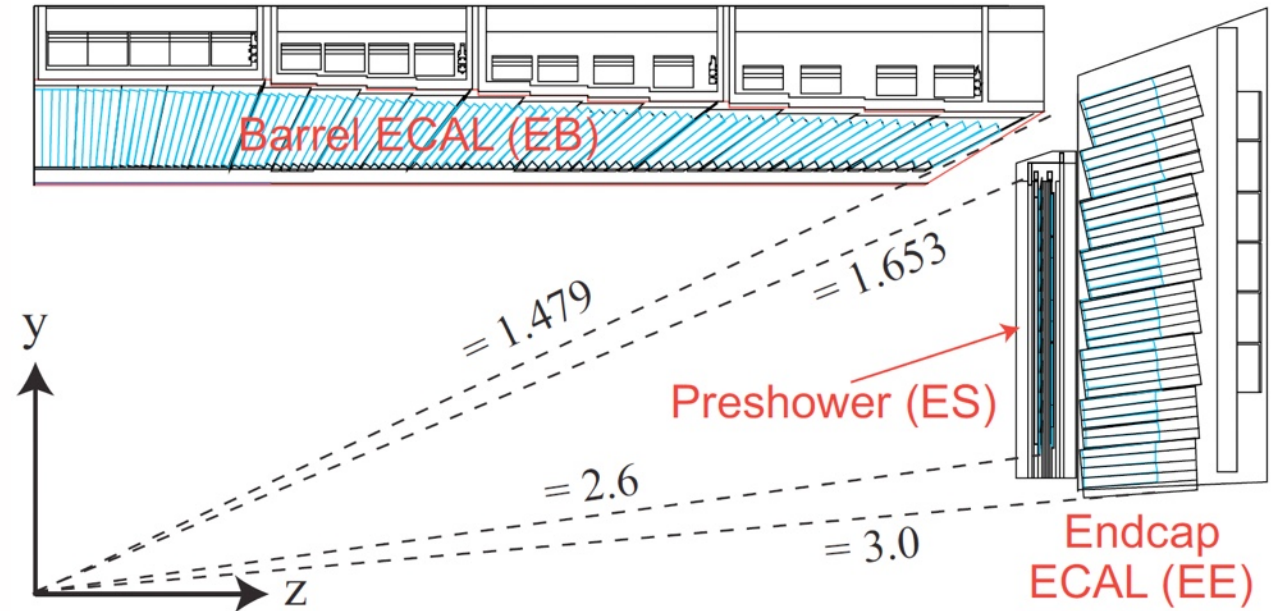
- CMS: PbWO_4 crystal calorimeter
- ATLAS: Lead/Liquid Argon (LAr) sampling calorimeter

ATLAS

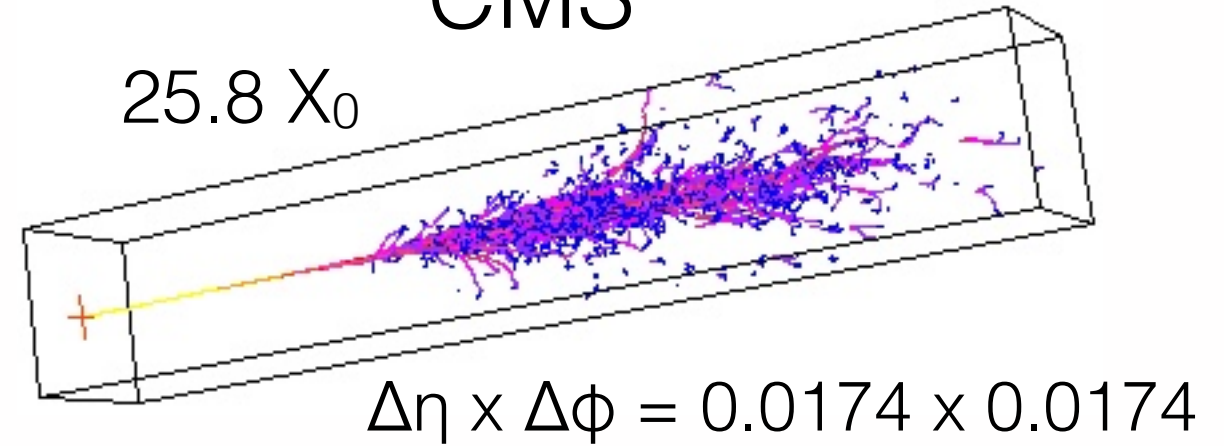




ATLAS



CMS

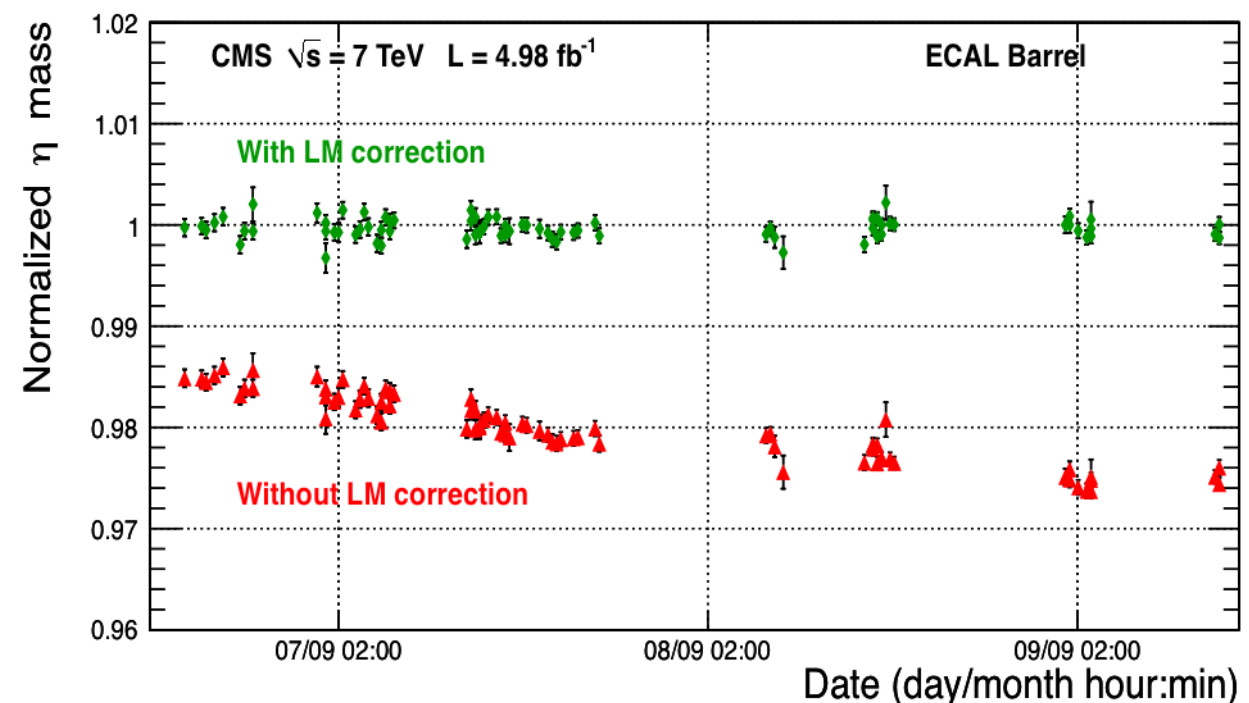
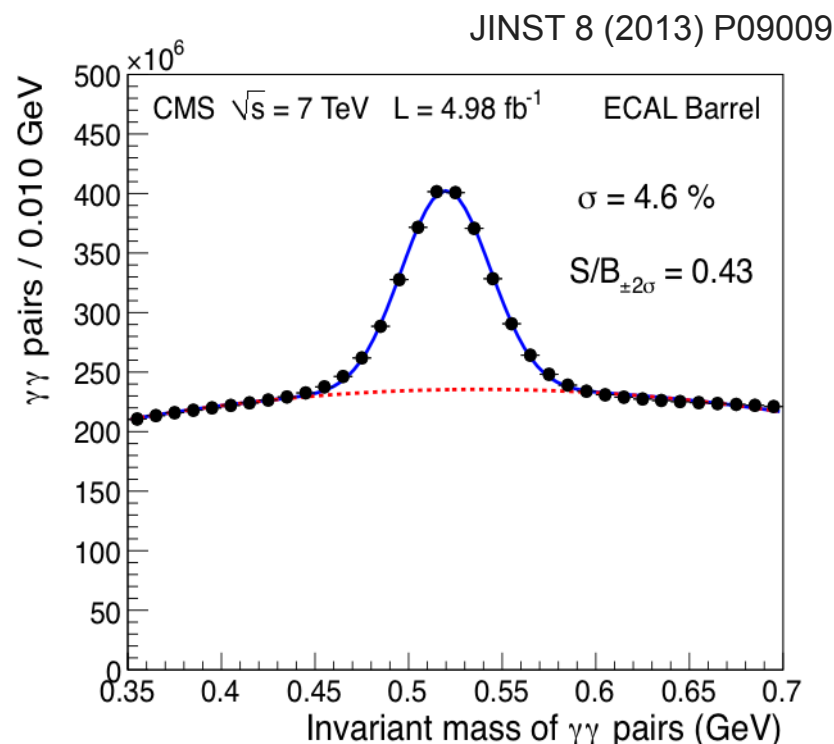
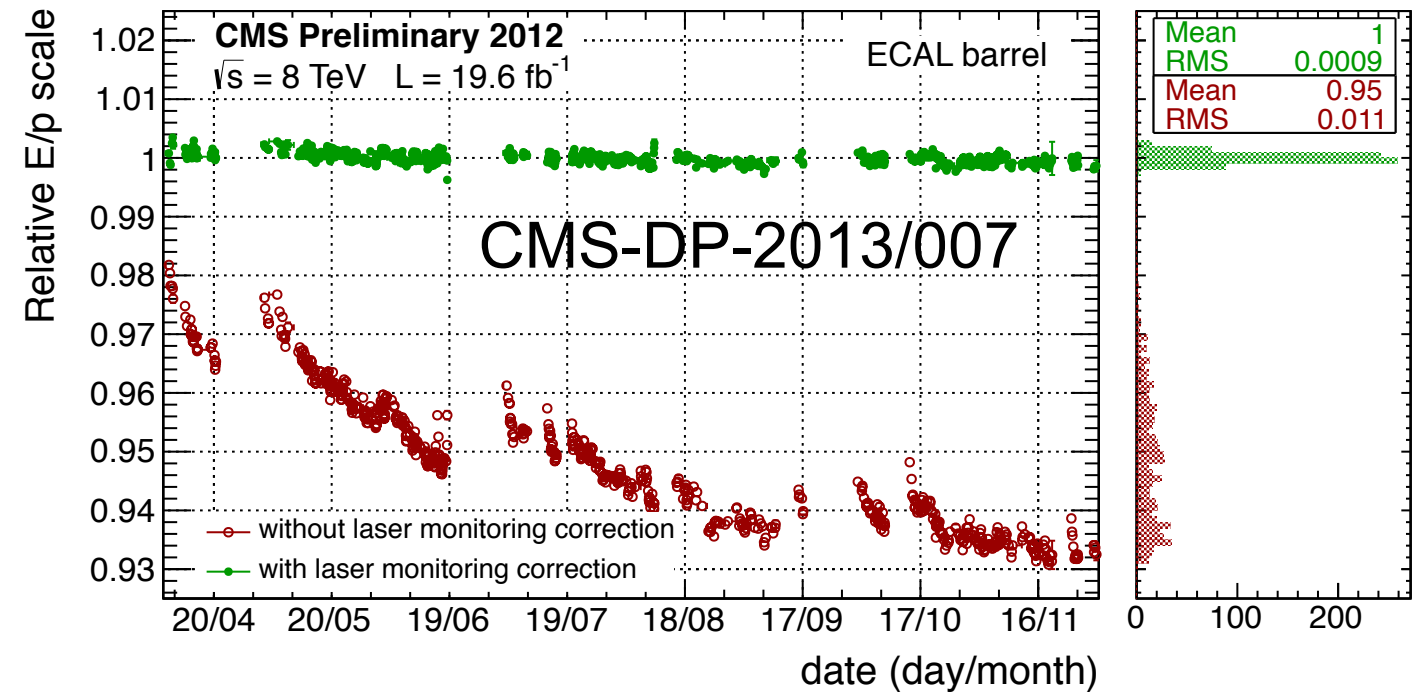


$$\frac{\sigma_E}{E} = \frac{10\%}{\sqrt{E}} \oplus 0.7\%$$

$$\frac{\sigma_E}{E} = \frac{2.8\%}{\sqrt{E}} \oplus 0.3\%$$

Intrinsic calorimeter resolution is not the whole story!

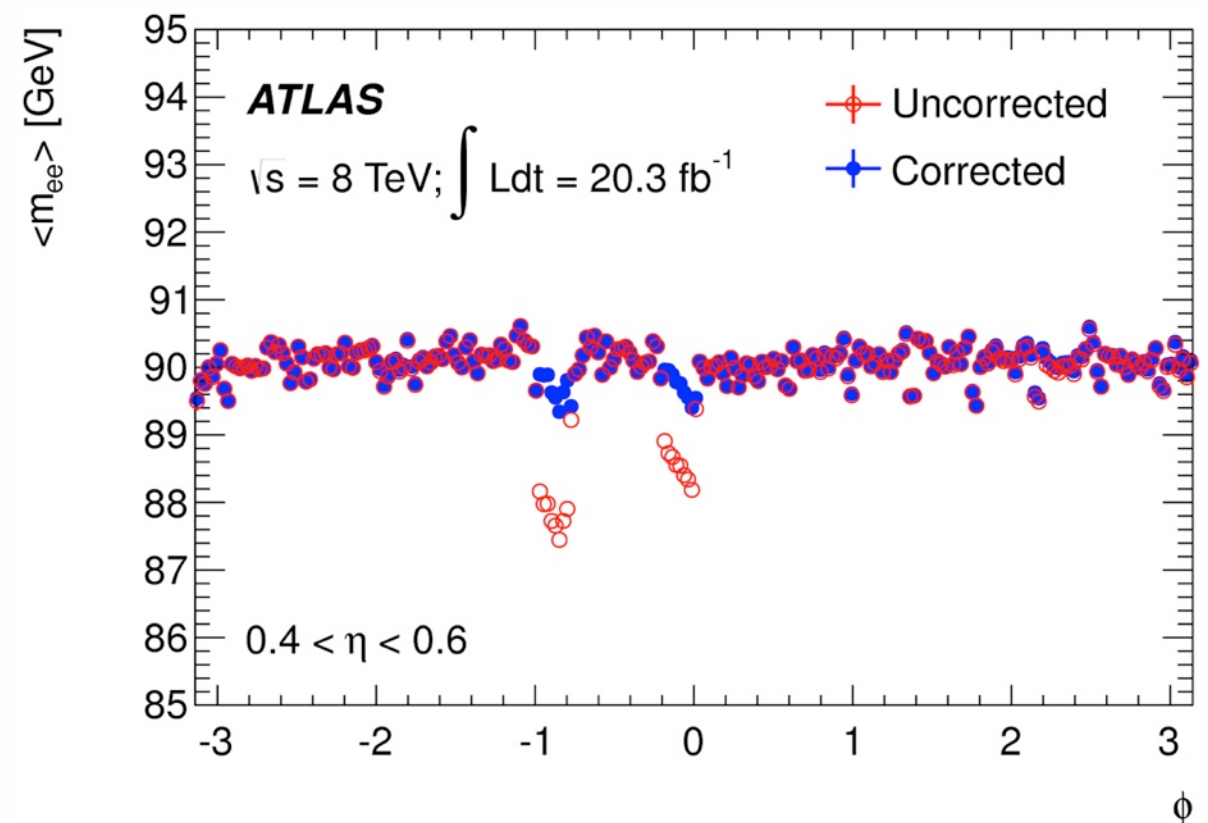
- Monitor variation of response vs. time with light monitoring (LM)
- π^0 and η decays
- φ -symmetry in minimum bias data
- E/p from isolated electrons in W/Z decays
- Crystal intercalibration uncertainties: 0.35% (1.6%) in most of the barrel (endcaps)



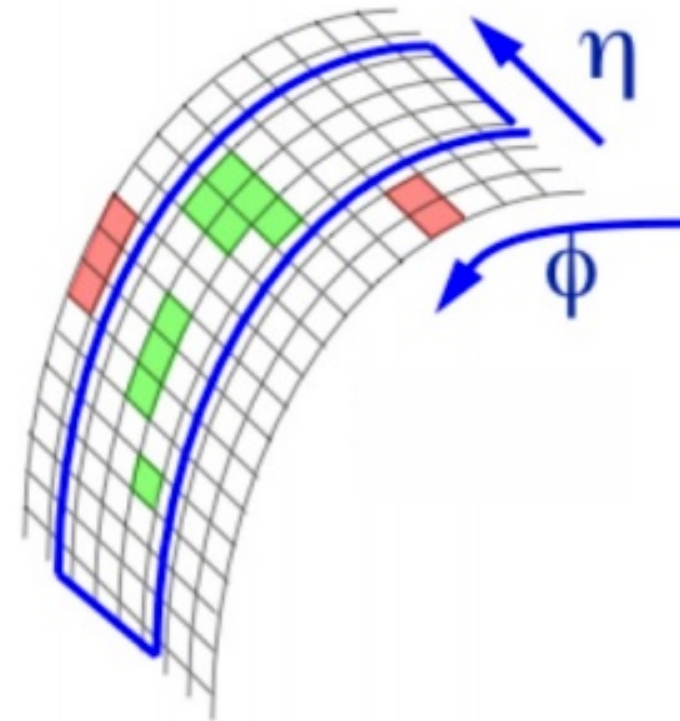
$$E_{\text{cell}} = F_{\mu\text{A} \rightarrow \text{MeV}} \times F_{\text{DAC} \rightarrow \mu\text{A}} \times \frac{1}{\frac{M_{\text{phys}}}{M_{\text{cali}}}} \times G \times \sum_{j=1}^{N_{\text{samples}}} a_j (s_j - p)$$

$5 \times 25 \text{ ns time slices}$ (points to N_{samples})
 $\text{Electronic pedestal from dedicated calibration runs}$ (points to p)
 $\text{low, medium, and high gain}$ (points to G)
 $\text{Correct for difference between calibration and physical pulses}$ (points to $\frac{1}{\frac{M_{\text{phys}}}{M_{\text{cali}}}}$)

- Corrected for HV differences
- Sectors with short circuits
- Time-dependent presampler response
- Differing energy responses depending on gain
- E/p in W/Z tracks, φ -symmetry



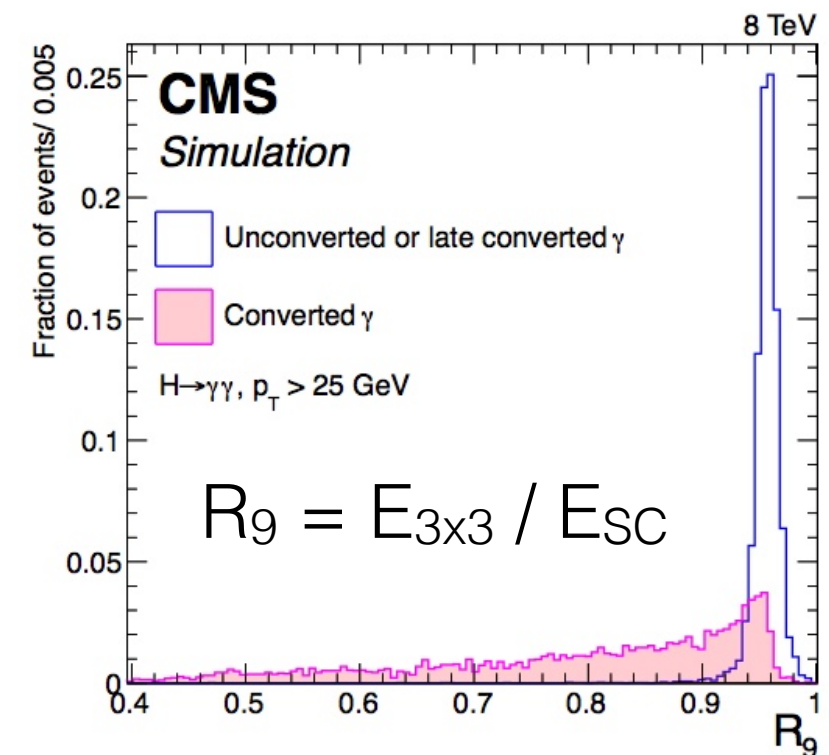
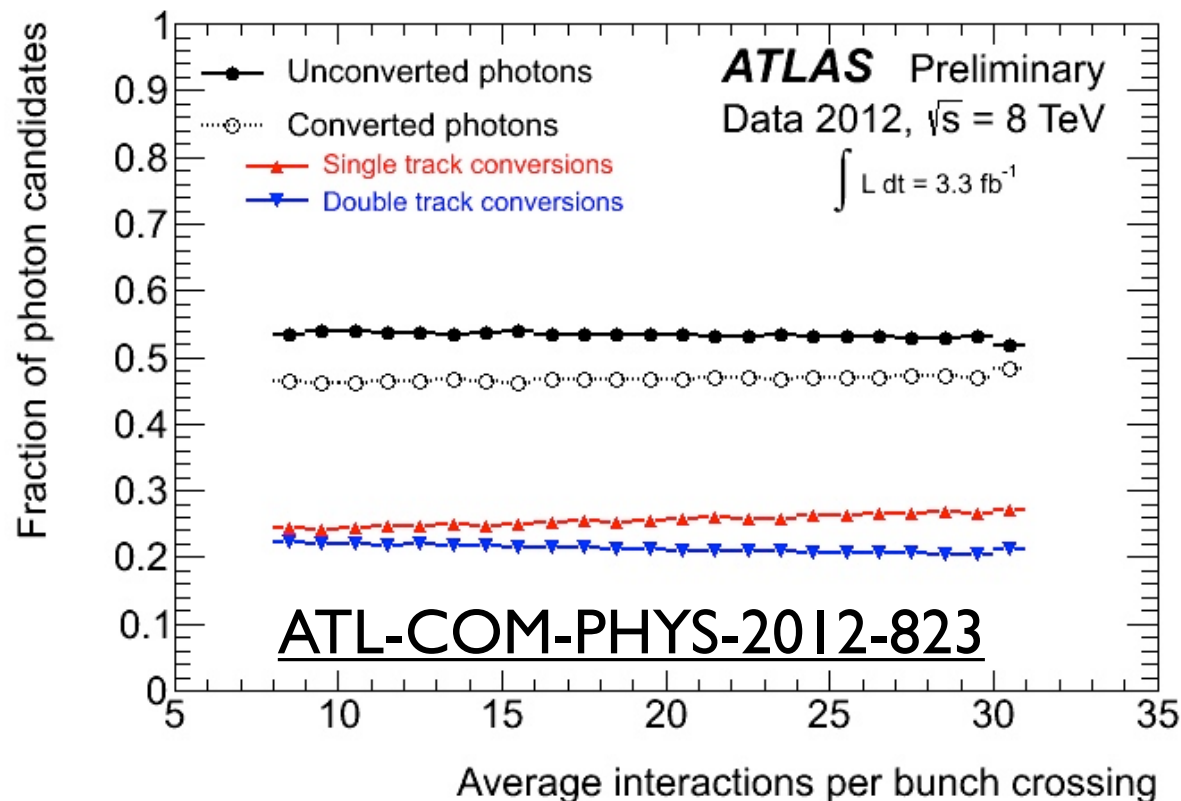
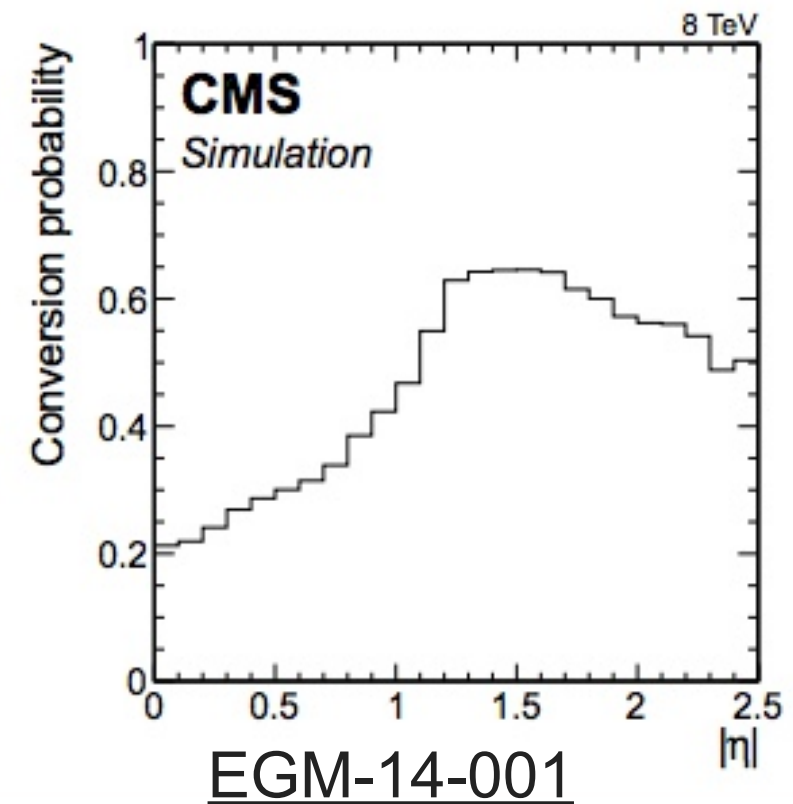
- For Run I, both experiments use $\eta \times \phi$ window algorithm
- CMS: if photon converts, large ϕ spread in strong B field
- Barrel superclusters (SC), made from 5×1 subclusters, may be extended up to 5×17
- Endcap: multiple 5×5 matrices, combined if overlapping
- ATLAS: precluster from middle layer, then sequentially seed clustering in other layers
- Choice between electrons and photon, and conversion-finding, to determine window size



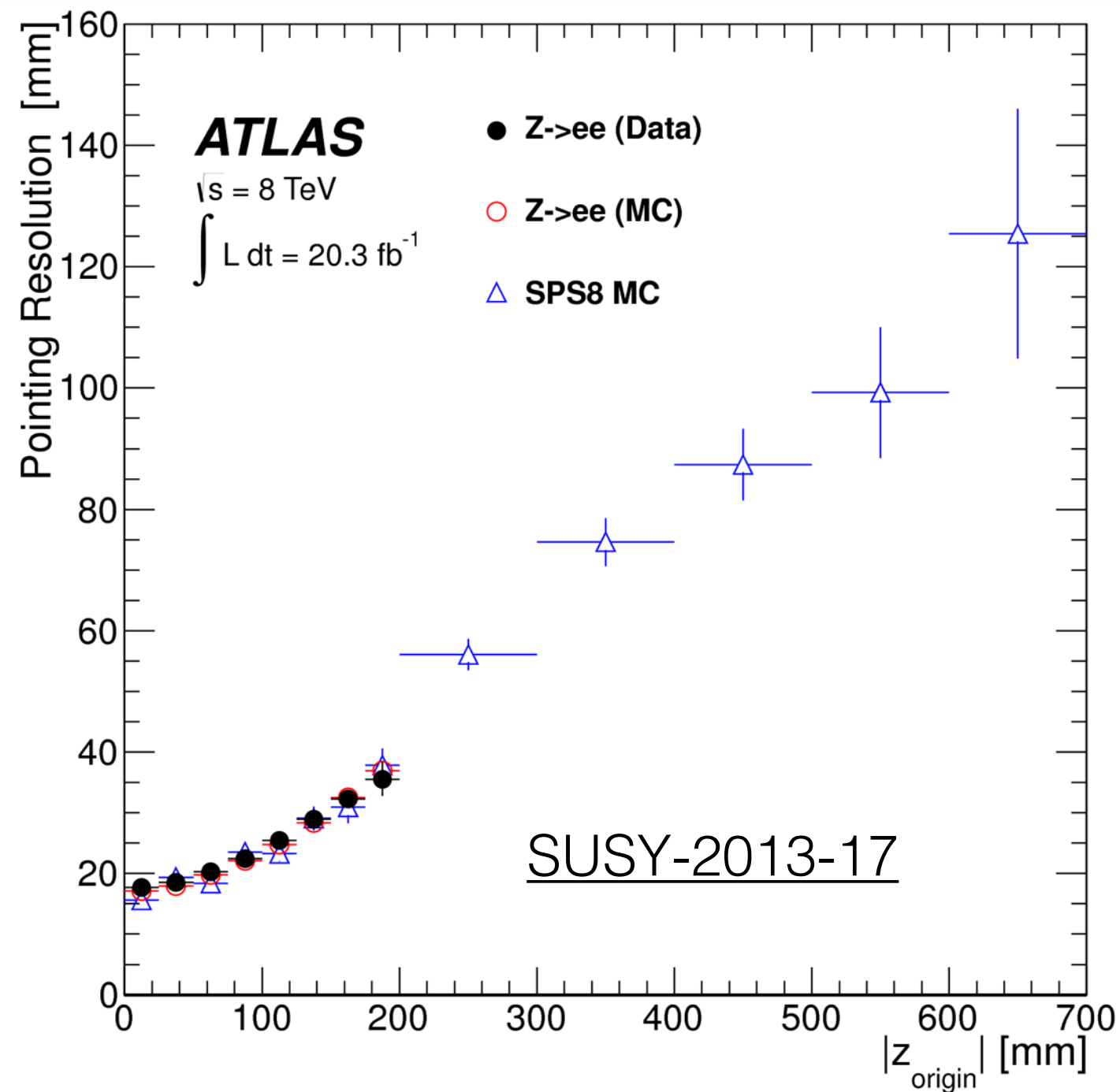
Order	Layer	$\Delta\eta_{cl}$ (units of 0.025)	$\Delta\phi_{cl}$ (units of 0.025)	Seed
1	Middle	$N_{\eta}^{cluster}$	$N_{\phi}^{cluster}$	$\eta_{precl}, \phi_{precl}$
2	Strips	$N_{\eta}^{cluster}$	6 or 8*	$\eta_{middle}, \phi_{middle}$
3	PS	$N_{\eta}^{cluster}$	6 or 8*	$\eta_{strips}, \phi_{strips}$
4	Back	$N_{\eta}^{cluster} + 1$	$N_{\phi}^{cluster}$	$\eta_{middle}, \phi_{middle}$

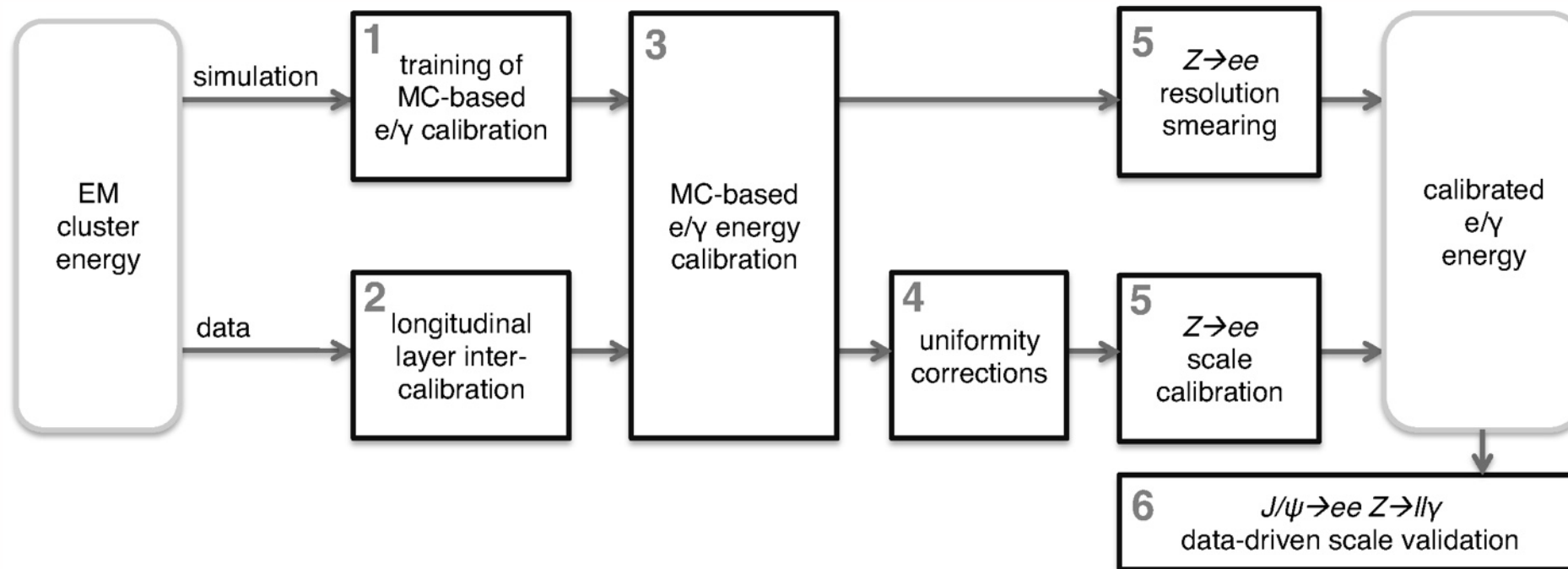
Particle Type	Barrel	Endcap
Electron	3×7	5×5
Converted photon	3×7	5×5
Unconverted photon	3×5	5×5

- CMS relies primarily on R_9 variable to identify photons that can be well-measured in ECAL
- ATLAS uses explicit conversion track reconstruction, benefits from electron ID in TRT



- Identification of correct vertex is vital
- For diphoton mass resolution in $H \rightarrow \gamma\gamma$ analysis
- For long-lifetime particle searches
- ATLAS has direct pointing information from electromagnetic calorimeter
- Beyond this, for $H\gamma\gamma$ both experiments use MVA's with similar information to select vertex (details in $H\gamma\gamma$ talk, P. Musella)

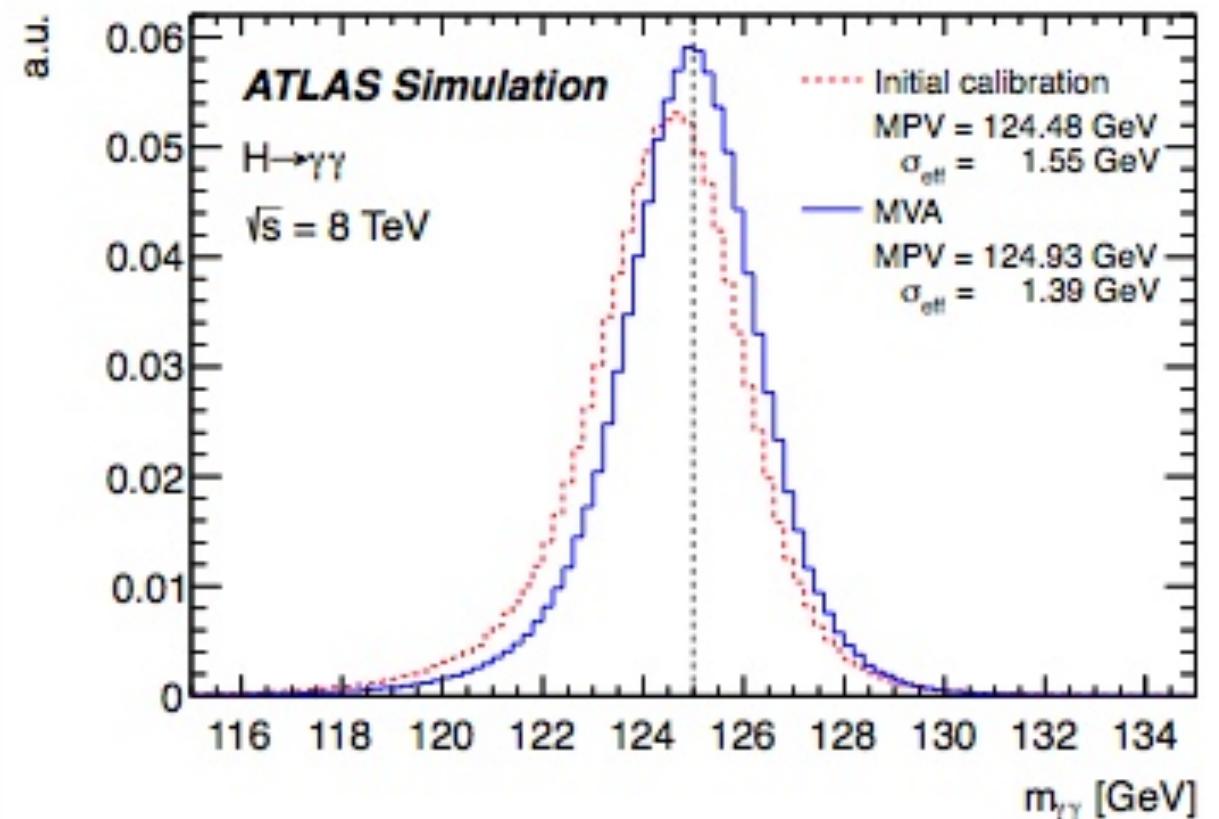
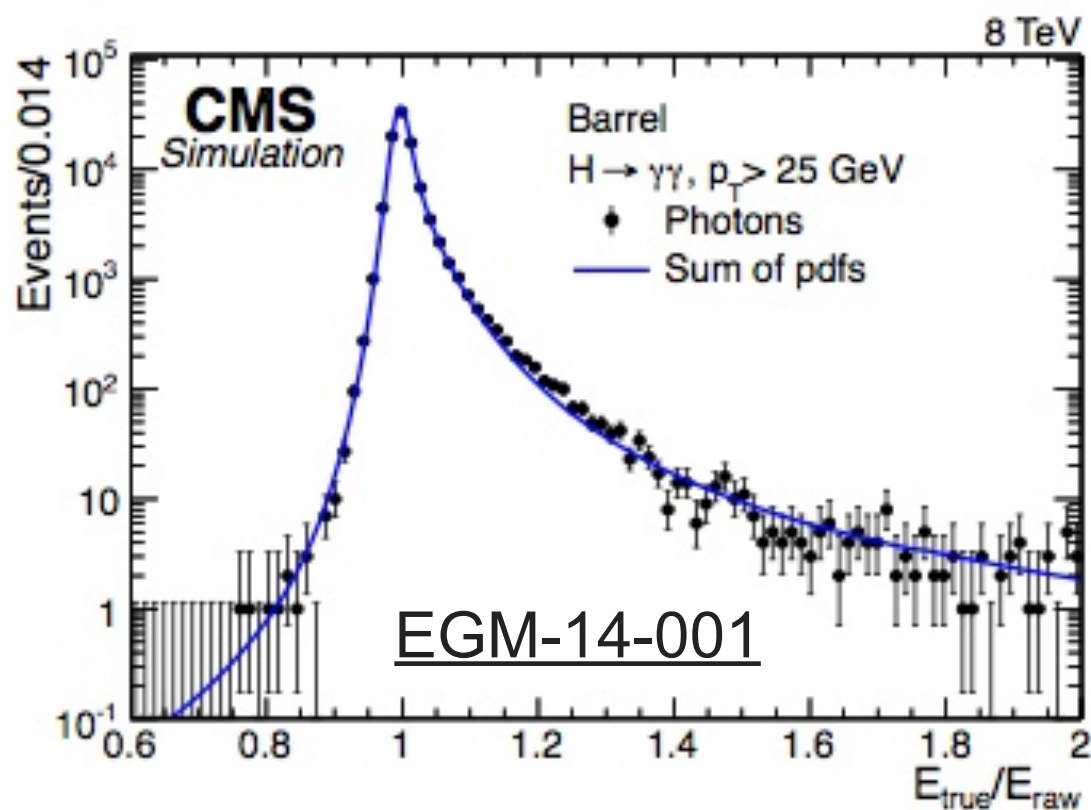


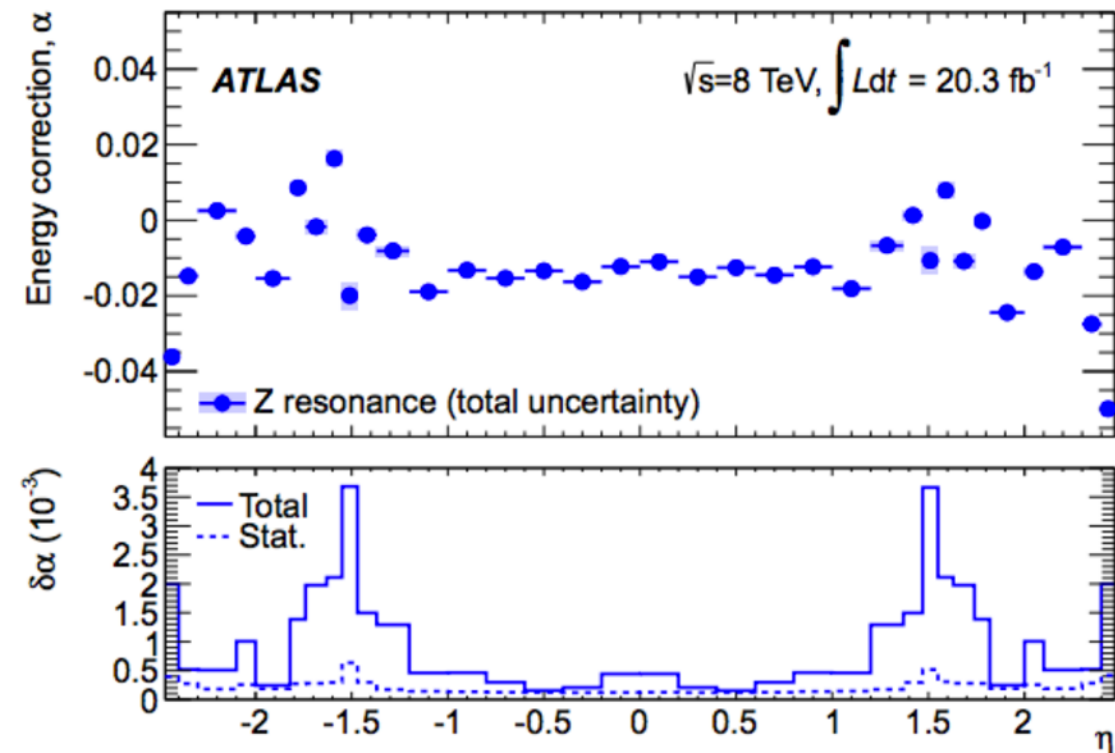
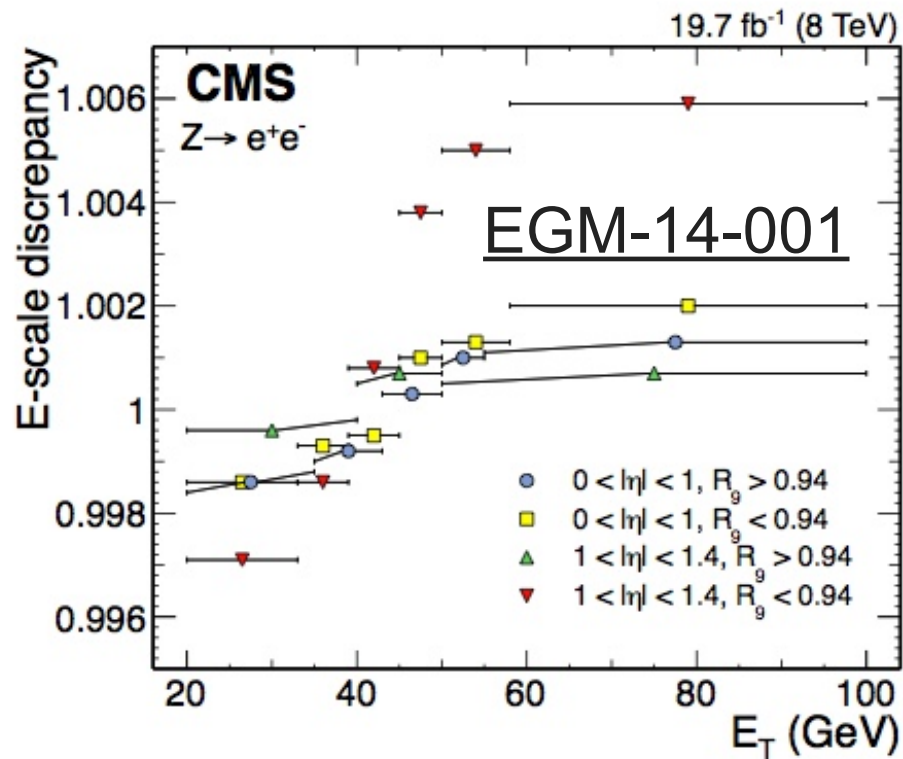


ATLAS

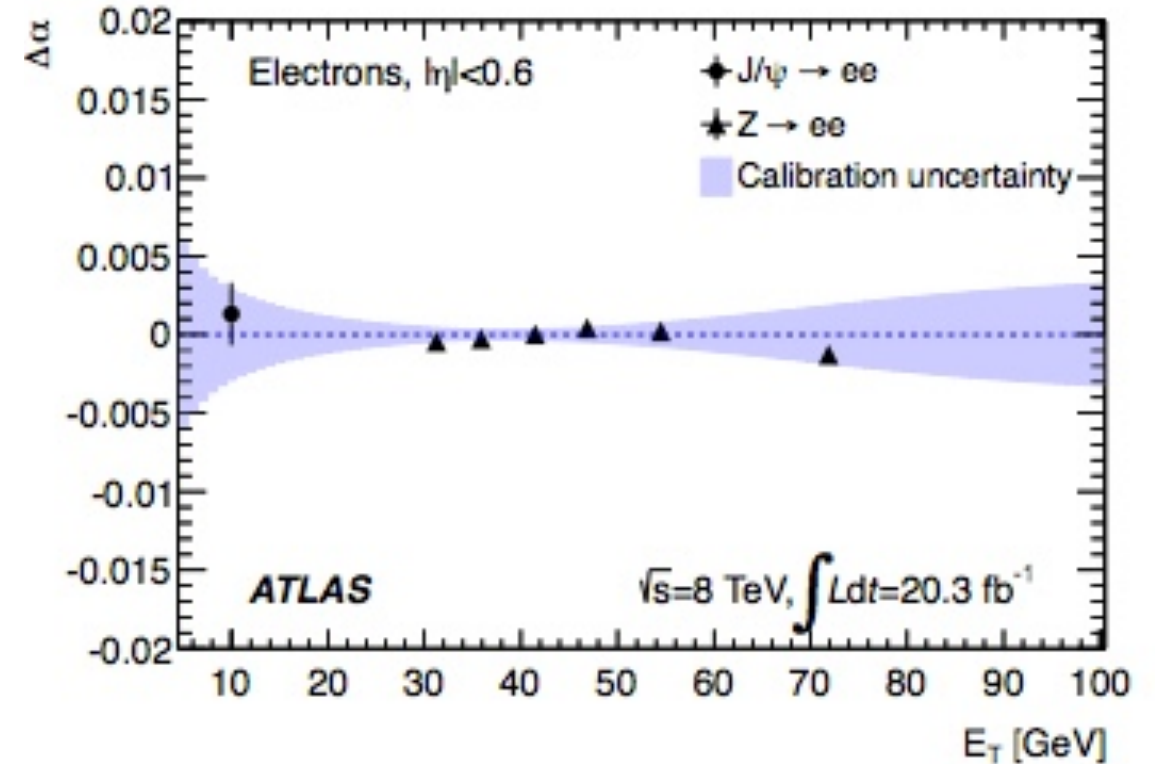
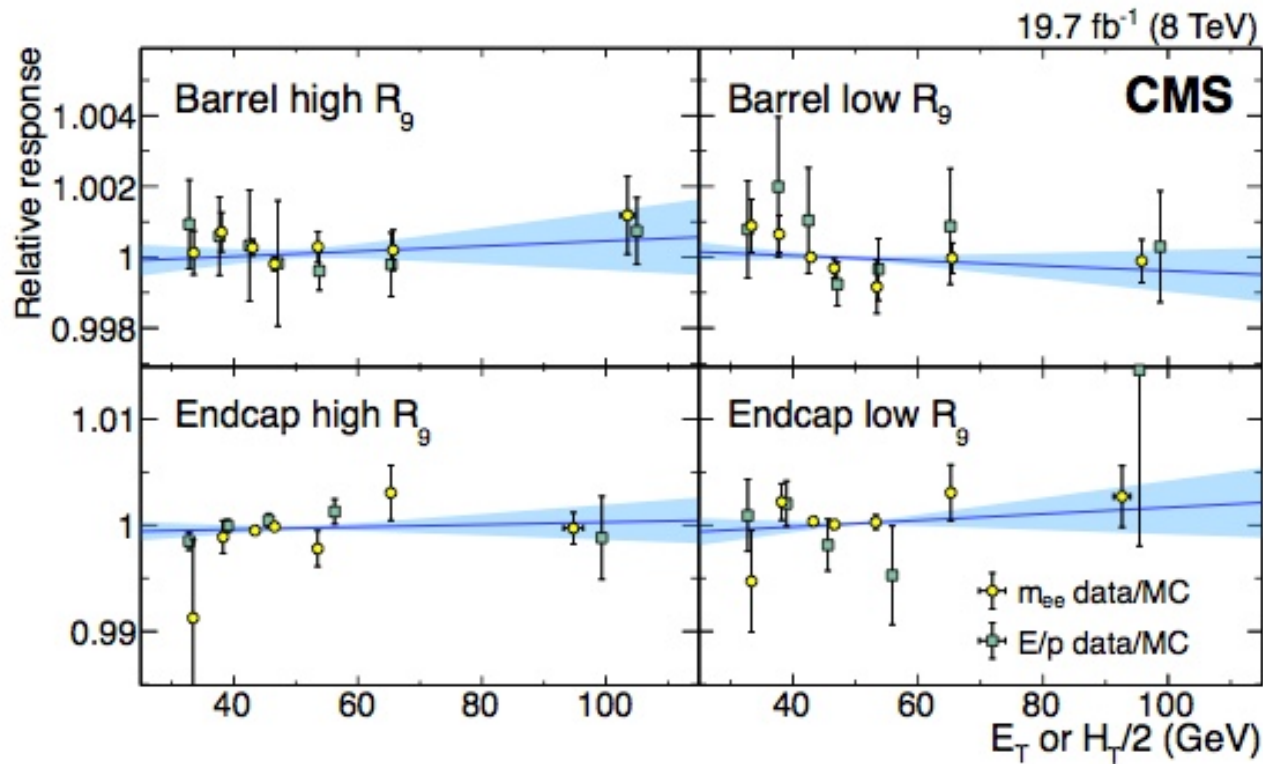
- CMS strategy similar
 - Semi-parametric MVA trained on MC
 - Fine-tuning of scale corrections with $Z \rightarrow ee$
 - Resolution smearing
 - Material studies and cross checks

- Both ATLAS and CMS use MVA to correct initial cluster energy
- Inputs
 - Raw energy, η , φ
 - CMS: Position w.r.t. edges of cells, modules, supermodules: different gap sizes
 - Shower widths
 - Energy ratios between smaller and larger areas (e.g. R9)
 - Energy ratio between layers (ATLAS only) or with preshower

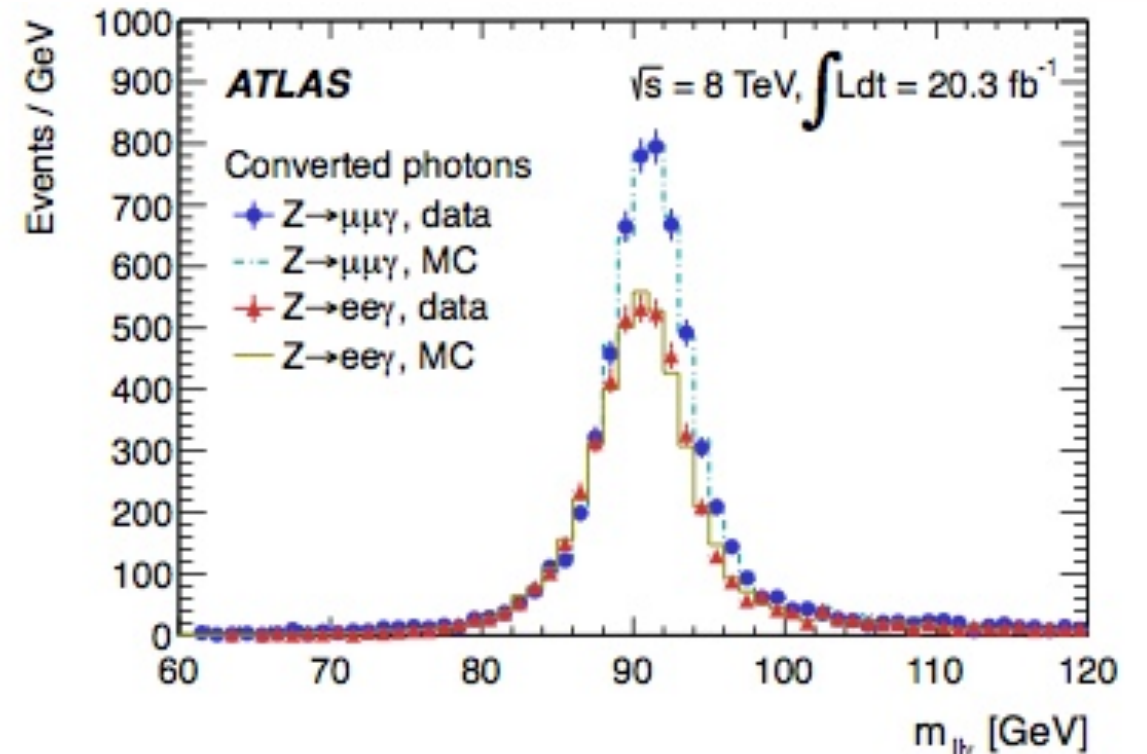




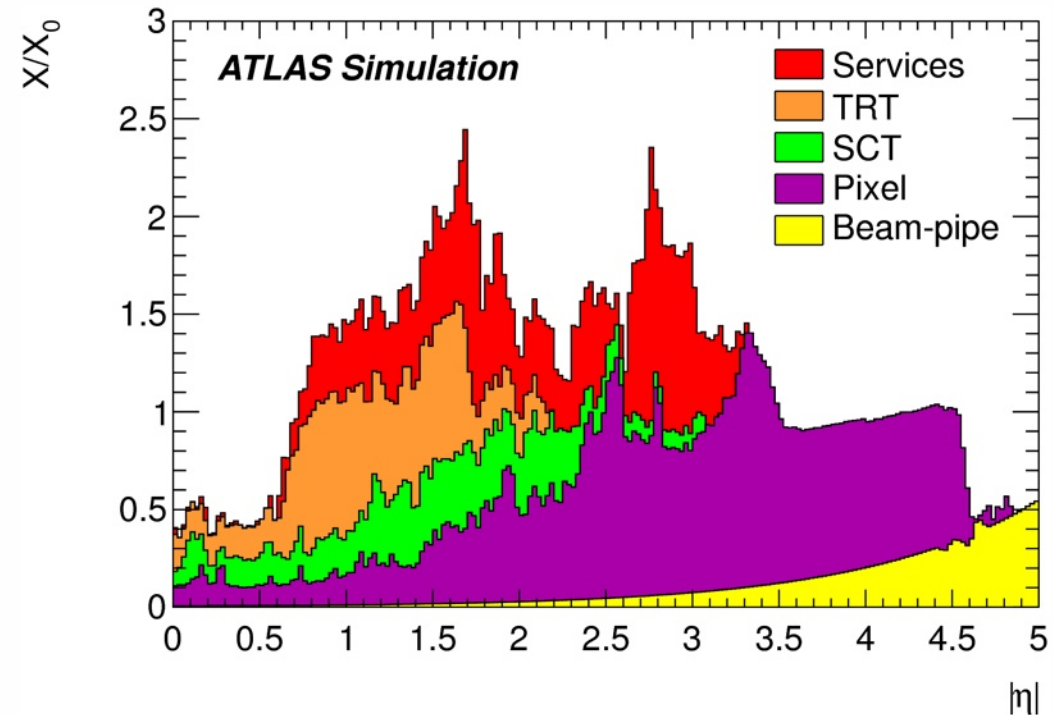
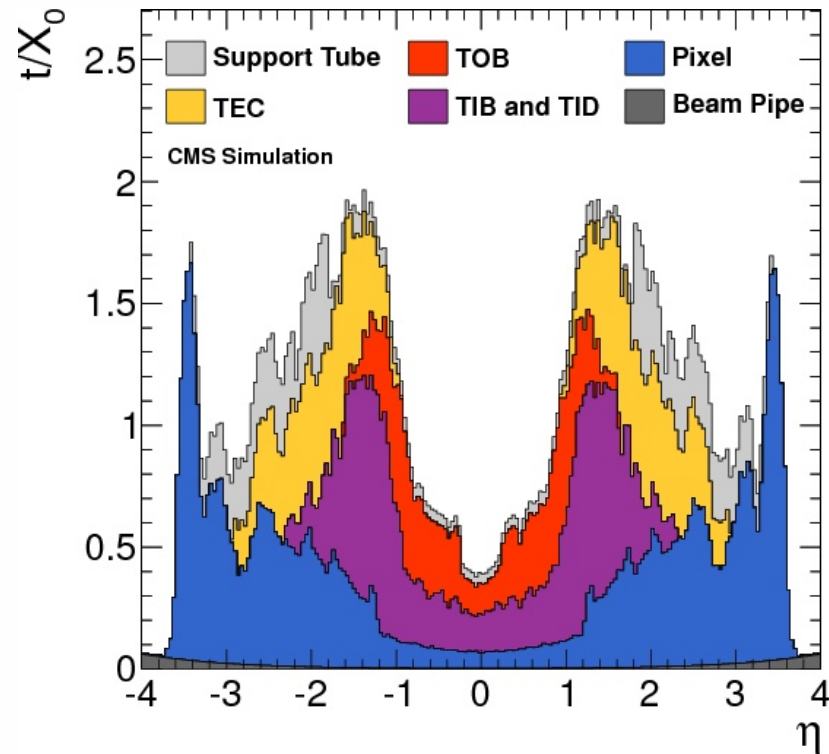
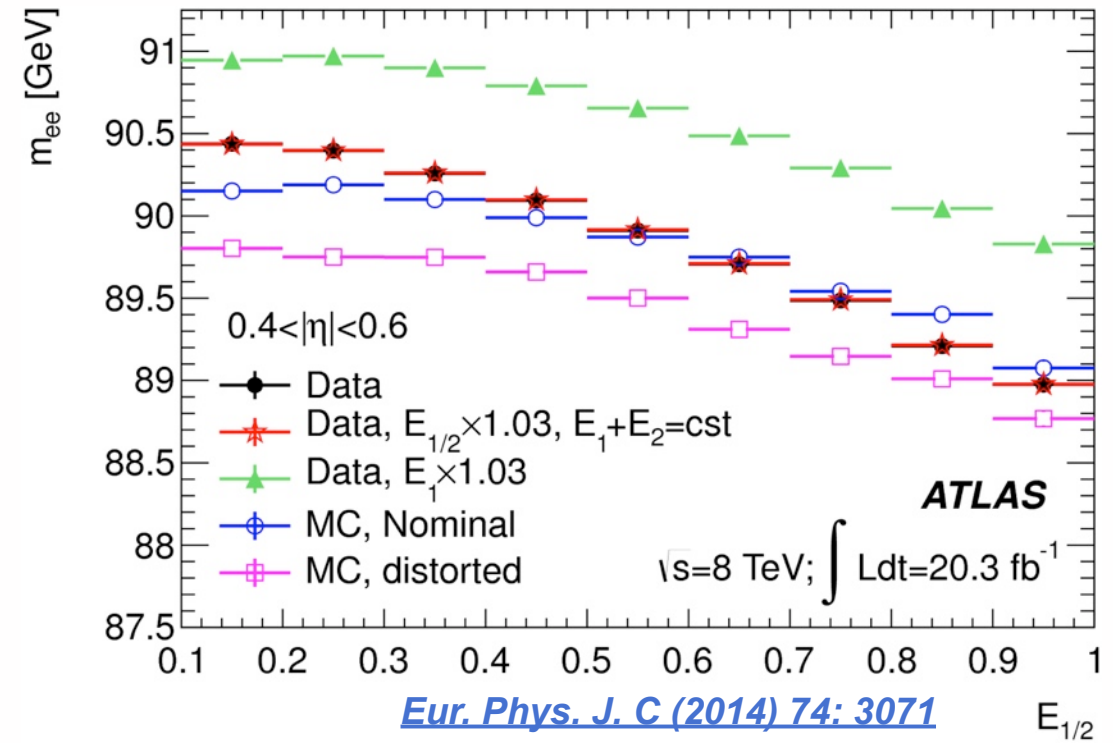
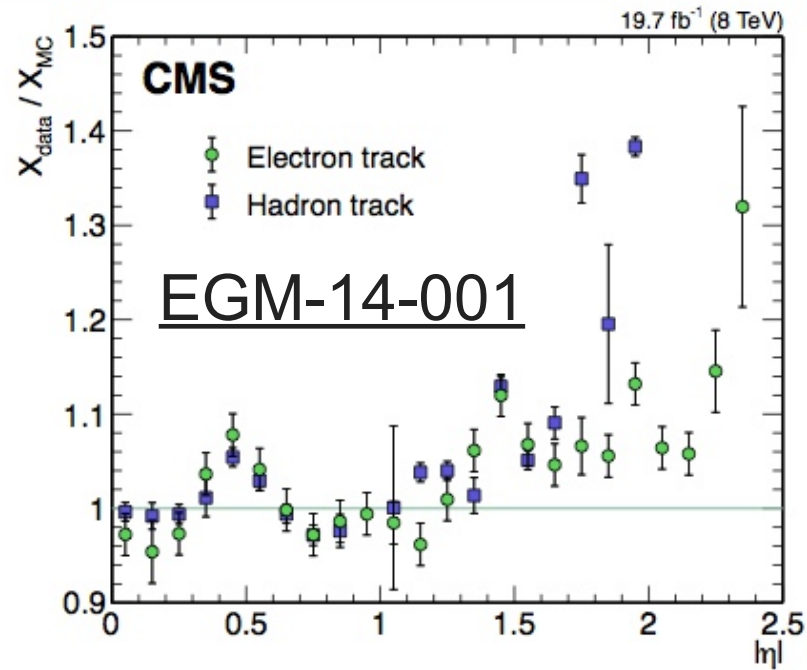
- CMS: 3 residual energy scale steps
 - 1st: residual time-dependence from E/p: changes of $< 0.1\%$ (0.2%) in barrel (endcap)
 - 2nd: $Z \rightarrow ee$ in R9 and η bins, mainly for material: corrections $< 1\%$
 - 3rd: E_T -dependent corrections, top left plot
- ATLAS: overall corrections: $< 2\%$ overall, uncertainly generally $\sim 0.05\%$ (top right)
- Additional smearing applied to MC to give agreement with $Z \rightarrow ee$ shape
 - CMS: 0.7% - 1% (1% - 2%) in barrel [$\pm 0.1\%$] for high (low) R9, 1.6% - 2.0% for endcaps [$\pm 0.3\%$ - 1.0%]
 - ATLAS: 0.8% [$\pm 0.3\%$] for barrel, 1.0% [$\pm 0.5\%$ for endcap]

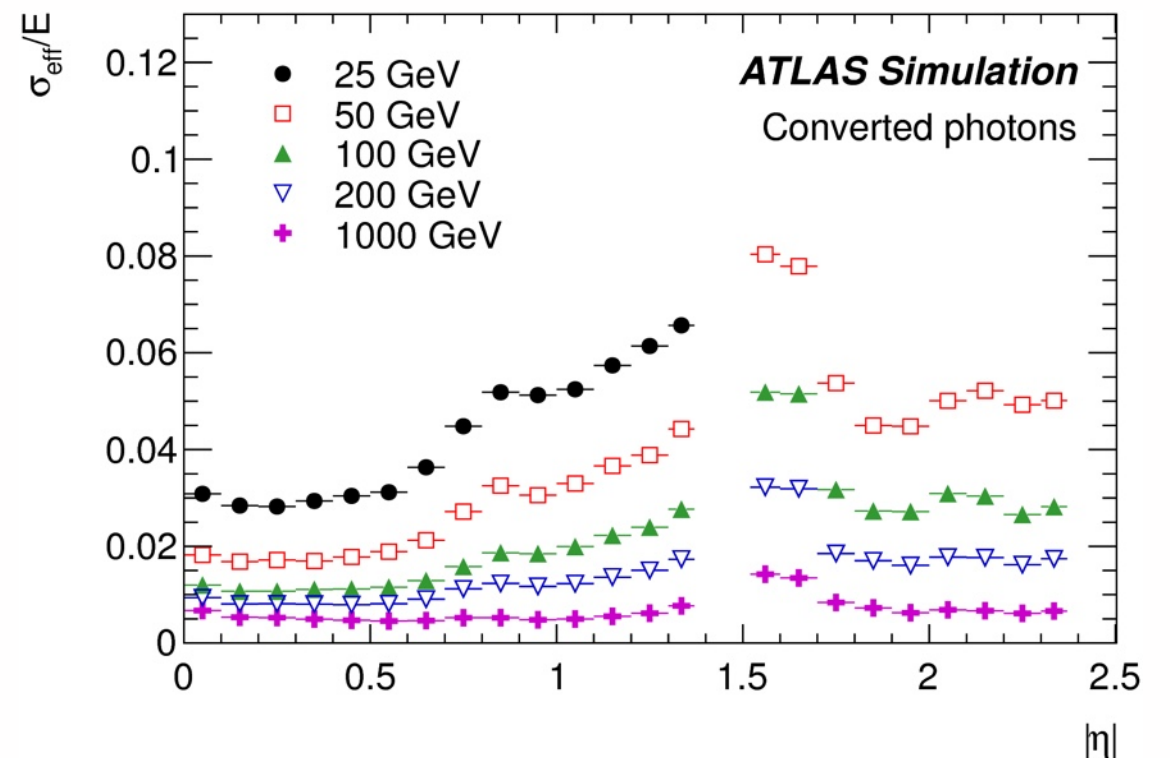
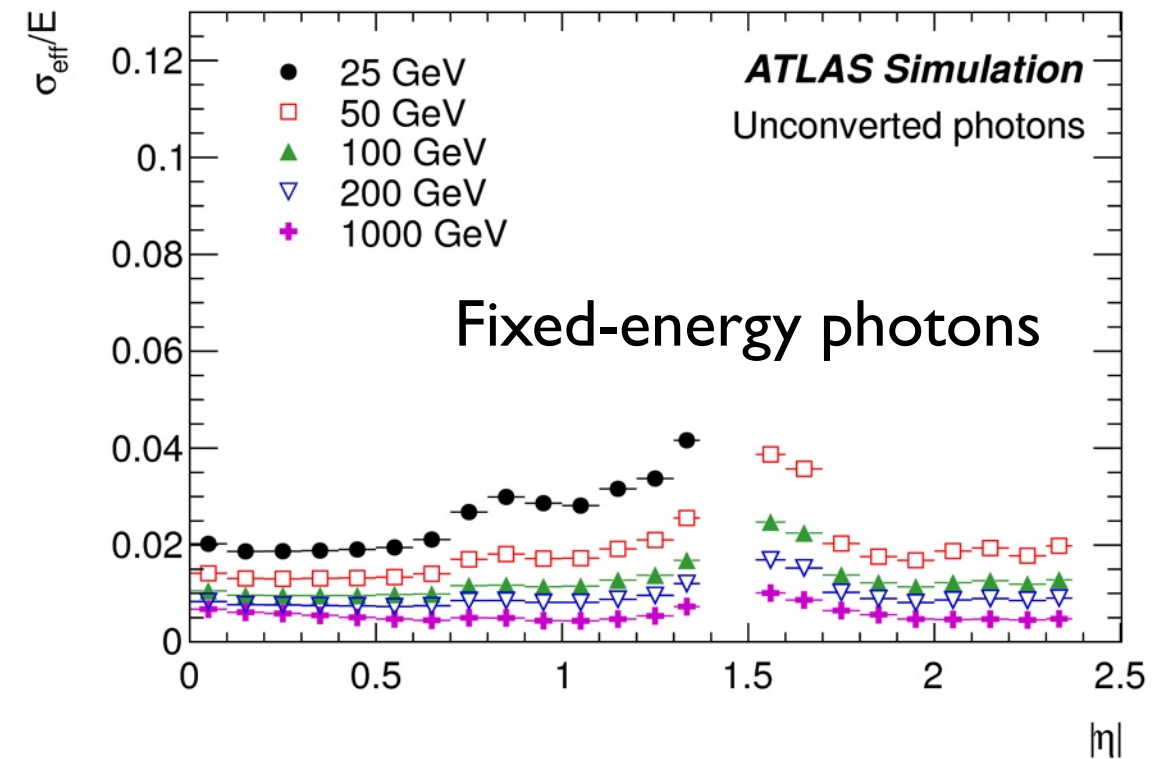
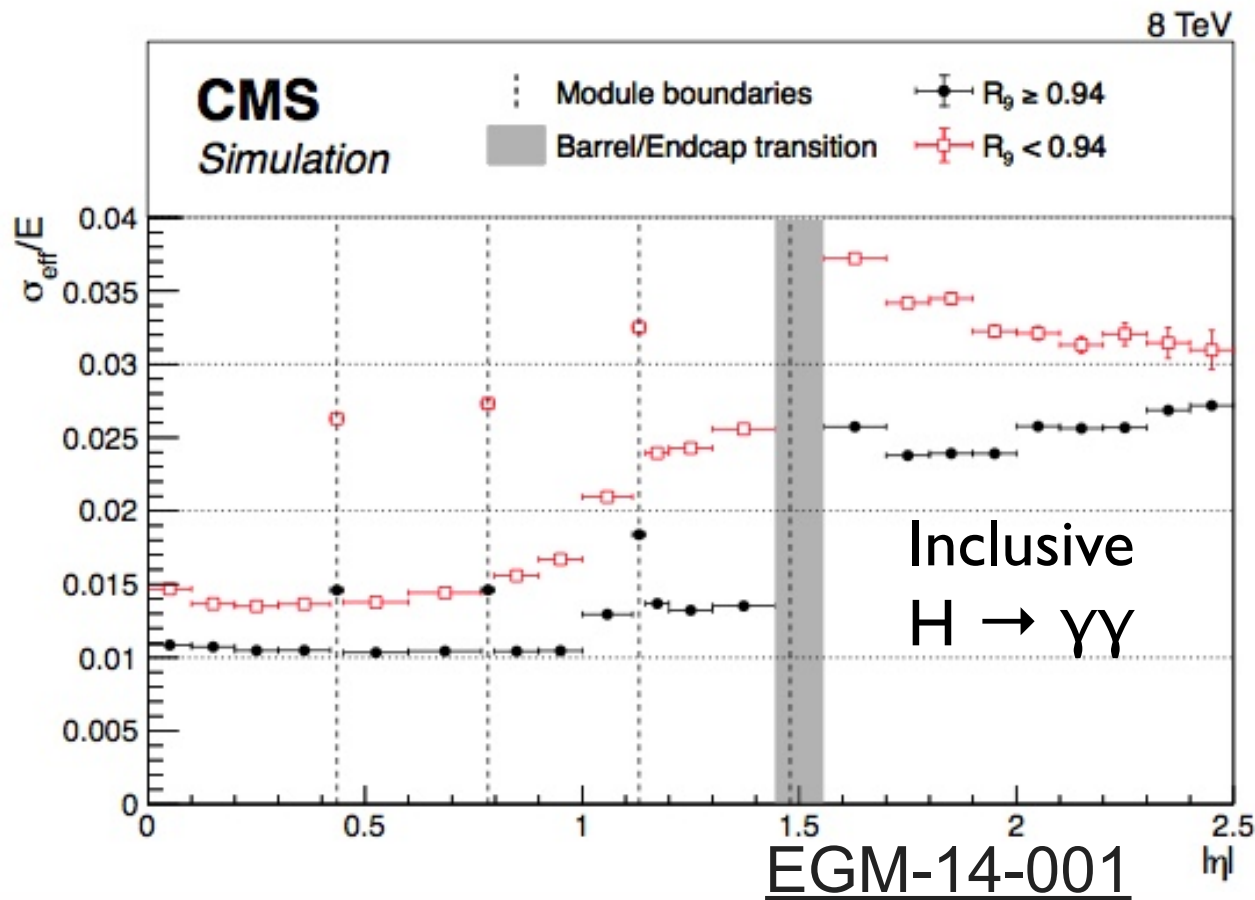


- Studies of $Z \rightarrow \ell\ell\gamma, J/\Psi \rightarrow \ell\ell$
- Major uncertainty: extrapolation away from $Z \rightarrow ee$ energy spectrum
- Material: next slide



- Material has a significant impact on resolution, accurate determination is vital





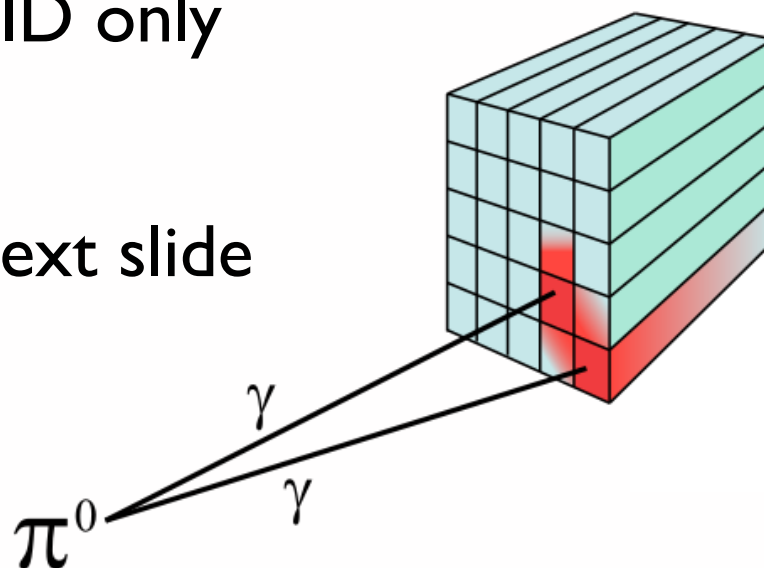
- Simulation results shown for:
 - CMS: Photons from $H \rightarrow \gamma\gamma$ events as selected in $H \rightarrow \gamma\gamma$ analysis
 - ATLAS: Fixed-energy photons

- Electron rejection: veto track match (excl. conversions)
- Efficiencies of CMS vetoes at right

CMS	Barrel		Endcap	
	γ	e	γ	e
Conversion-safe veto	$99.1 \pm 0.1\%$	5.3%	$97.8 \pm 0.2\%$	19.6%
Pixel track seed veto	$94.4 \pm 0.2\%$	1.4%	$81.0 \pm 0.6\%$	4.3%

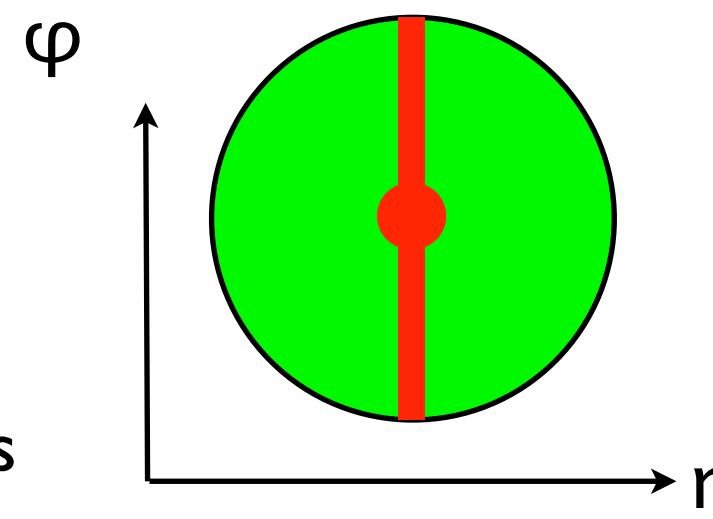
- Shower shape variables
 - ATLAS example at right
 - Strip layer variables used in tight ID only

EM Middle layer	Ratio in η of cell energies in 3×7 versus 7×7 cells	R_η
	Lateral width of the shower	$w_{\eta 2}$
	Ratio in ϕ of cell energies in 3×3 and 3×7 cells	R_ϕ
EM Strip layer	Shower width for three strips around strip with maximum energy deposit	$w_{s 3}$
	Total lateral shower width	$w_{s \text{ tot}}$
	Energy outside core of three central strips but within seven strips divided by energy within the three central strips	F_{side}
	Difference between the energy associated with the second maximum in the strip layer, and the energy reconstructed in the strip with the minimal value found between the first and second maxima	ΔE
	Ratio of the energy difference associated with the largest and second largest energy deposits over the sum of these energies	E_{ratio}



ATLAS

- CMS: separately use 3 isolation sums of PF objects within $\Delta R < 0.3$ of the photon
 - Charged hadrons, neutral hadrons, photons
 - *Exclude* nearby objects to avoid counting deposits assigned to photon:
 - $\Delta\eta < 0.015$ for PF photons,
 - $\Delta R < 0.02$ for charged hadrons
 - This will be changed in Run 2 (slide 24)
- ATLAS: isolation sum over all calorimeter cells
- Both experiments correct for the average energy from pileup (ρ) multiplied by effective area of photon candidate





- CMS: tight, medium and loose working points
- ATLAS: tight and loose working point cuts separately optimized based on presence of conversions in bins of depend on \square

CMS

		Loose	Medium	Tight
I_γ	barrel	1.3 GeV + 0.005 p_T^γ	0.7 GeV + 0.005 p_T^γ	0.7 GeV + 0.005 p_T^γ
	endcap	—	1 GeV + 0.005 p_T^γ	1 GeV + 0.005 p_T^γ
I_n	barrel	3.5 GeV + 0.04 p_T^γ	1.0 GeV + 0.04 p_T^γ	0.4 GeV + 0.04 p_T^γ
	endcap	2.9 GeV + 0.04 p_T^γ	1.5 GeV + 0.04 p_T^γ	1.5 GeV + 0.04 p_T^γ
I_π	barrel	2.6 GeV	1.5 GeV	0.7 GeV
	endcap	2.3 GeV	1.2 GeV	0.5 GeV
$\sigma_{\eta\eta}$	barrel	0.012	0.011	0.011
	endcap	0.034	0.033	0.031
f_h		0.05		
Electron veto		conversion-safe		

Category	Description	Name	Loose	Tight
Acceptance	$ \eta < 2.37, 1.37 < \eta < 1.52$ excluded	—	✓	✓
Hadronic leakage	Ratio of E_T in the first sampling of the hadronic calorimeter to E_T of the EM cluster (used over the range $ \eta < 0.8$ and $ \eta > 1.37$)	R_{had1}	✓	✓
	Ratio of E_T in all the hadronic calorimeter to E_T of the EM cluster (used over the range $0.8 < \eta < 1.37$)	R_{had}	✓	✓
EM Middle layer	Ratio in η of cell energies in 3×7 versus 7×7 cells	R_η	✓	✓
	Lateral width of the shower	$w_{\eta2}$	✓	✓
	Ratio in ϕ of cell energies in 3×3 and 3×7 cells	R_ϕ		✓
EM Strip layer	Shower width for three strips around strip with maximum energy deposit	w_{s3}		✓
	Total lateral shower width	w_{stot}		✓
	Energy outside core of three central strips but within seven strips divided by energy within the three central strips	F_{side}		✓
	Difference between the energy associated with the second maximum in the strip layer, and the energy reconstructed in the strip with the minimal value found between the first and second maxima	ΔE		✓
	Ratio of the energy difference associated with the largest and second largest energy deposits over the sum of these energies	E_{ratio}		✓

ATLAS

Table 1: Variables used for loose and tight photon identification cuts.

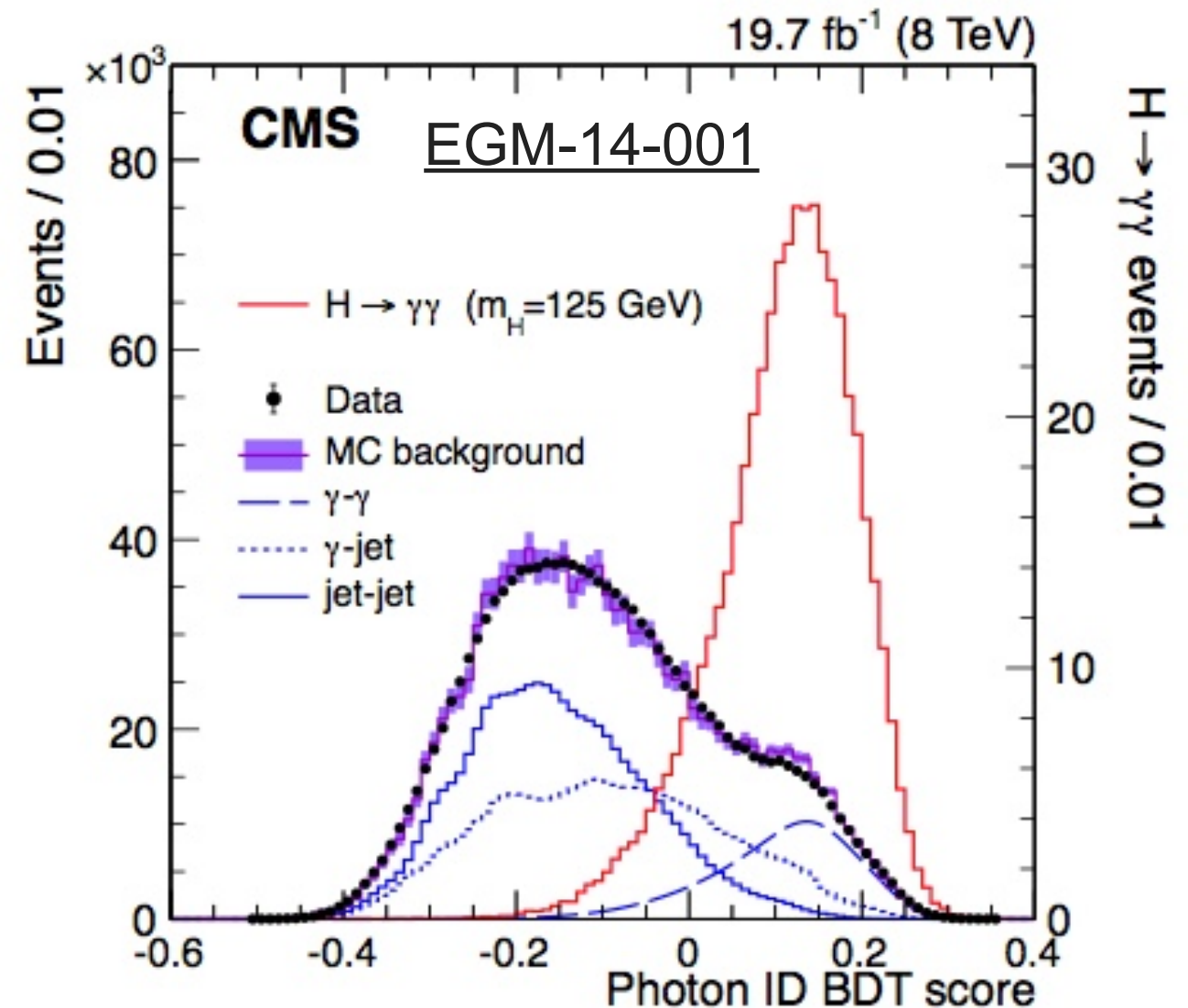
Preselection based on Trigger:

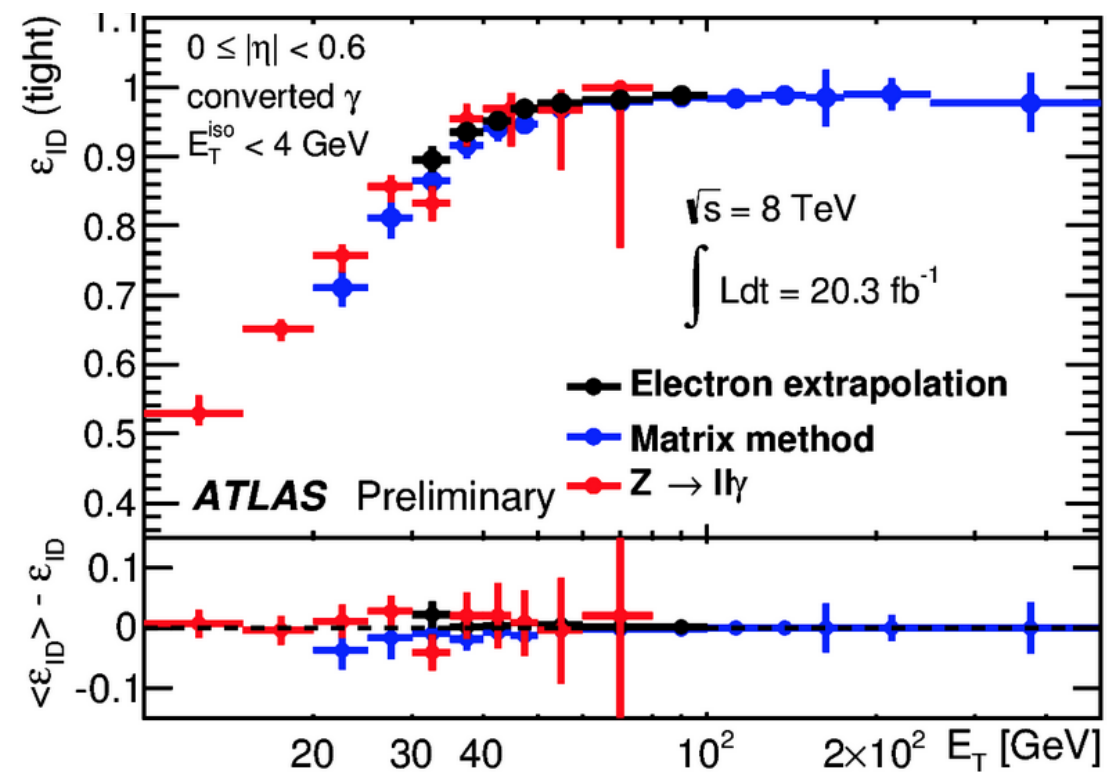
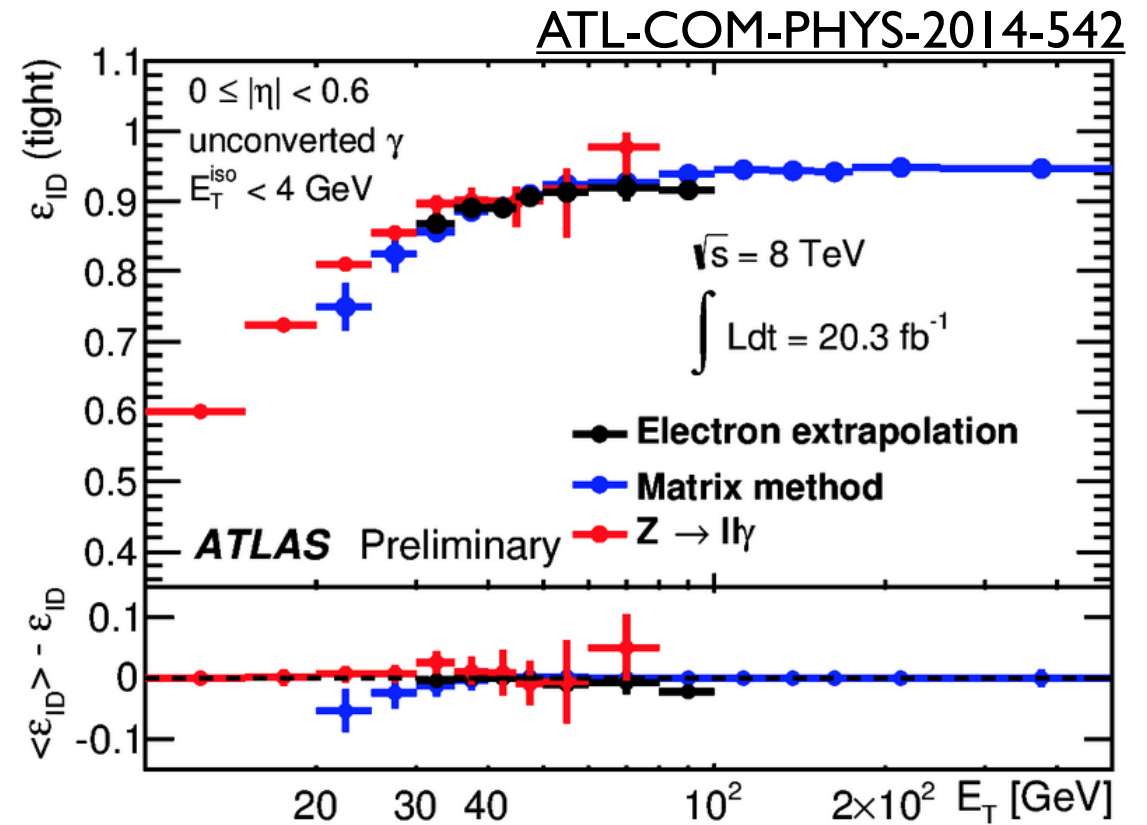
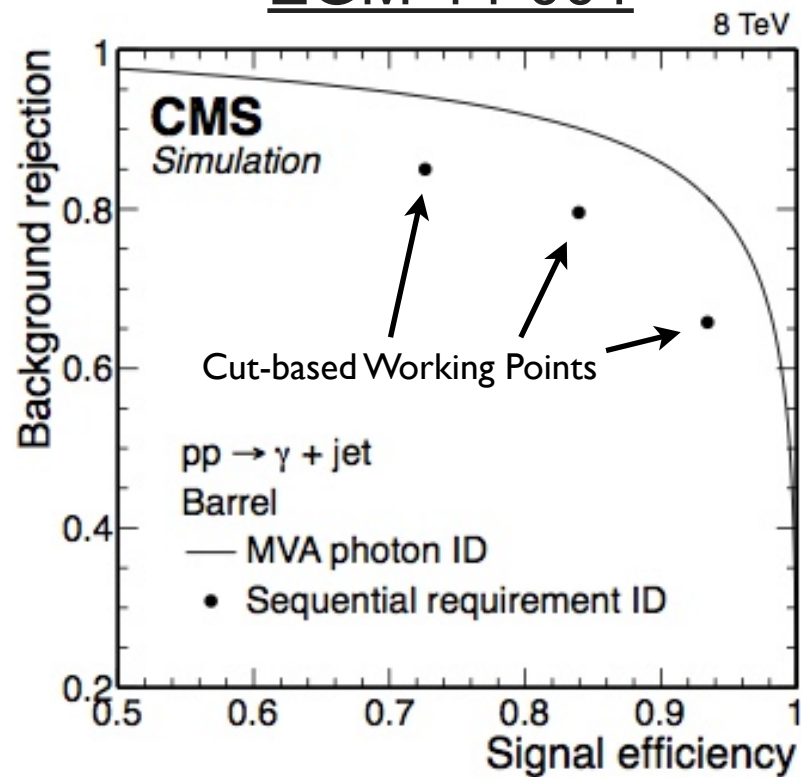
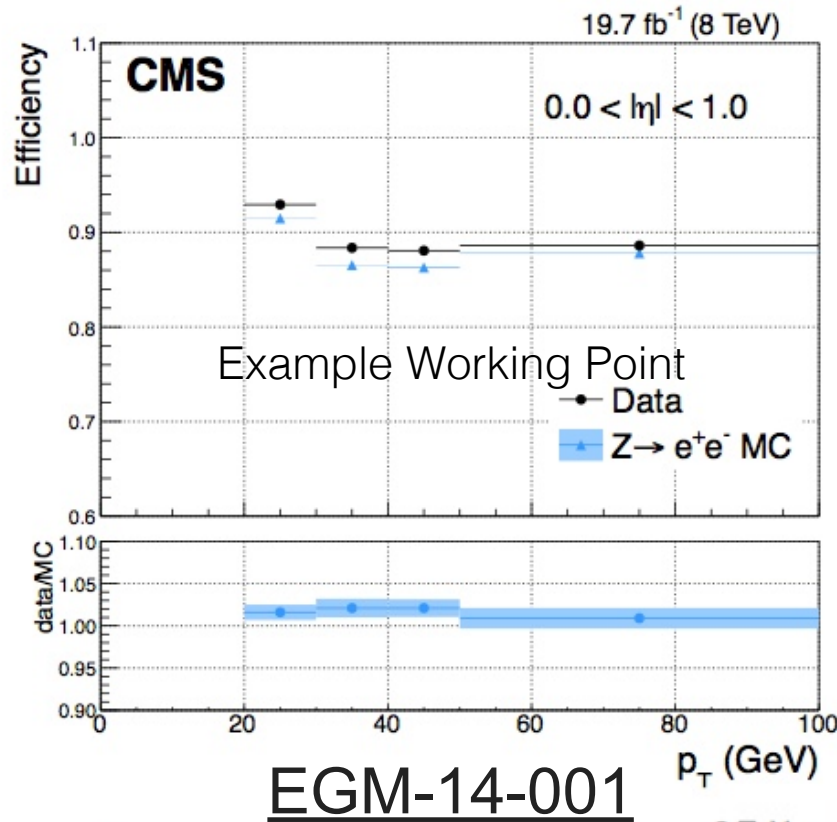
- For $H \rightarrow \gamma\gamma$ analysis
- Enables use of further variables that provide modest discrimination but cannot be easily used for cuts

- Photon isolation
- Charged isolation depends on vertex selection (details in $H \rightarrow \gamma\gamma$ talk, P. Musella)
 - Isolation w.r.t. chosen vertex
 - Isolation w.r.t. worst vertex
- 6 shape variables
- Width in preshower (endcap)
- $E, \rho, R9$

Table 3: Preselection requirements used for the $H \rightarrow \gamma\gamma$ analysis.

R_9	f_h		$\sigma_{\eta\eta}$		I_{HCAL}	I_{Trk}	I_{π}
	barrel	endcap	barrel	endcap			
≤ 0.9	< 0.075	< 0.075	< 0.014	< 0.034	$< 4 \text{ GeV}$	$< 4 \text{ GeV}$	$< 4 \text{ GeV}$
> 0.9	< 0.082	< 0.075	< 0.014	< 0.034	$< 50 \text{ GeV}$	$< 50 \text{ GeV}$	$< 4 \text{ GeV}$

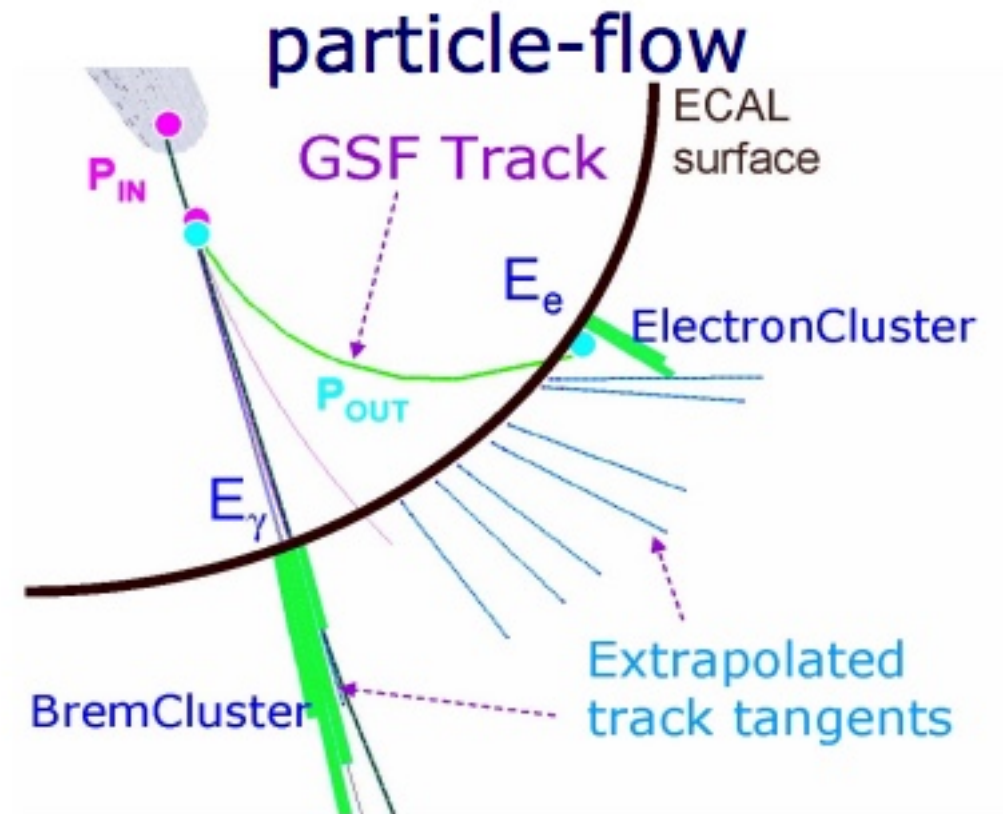




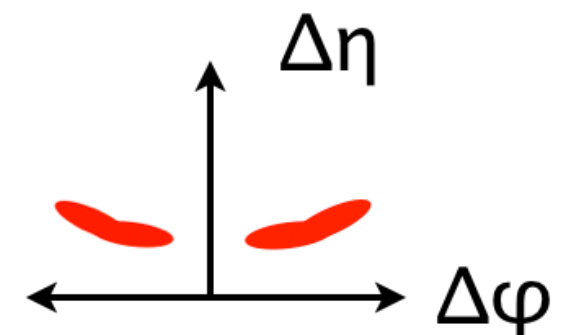


Looking toward Run 2...

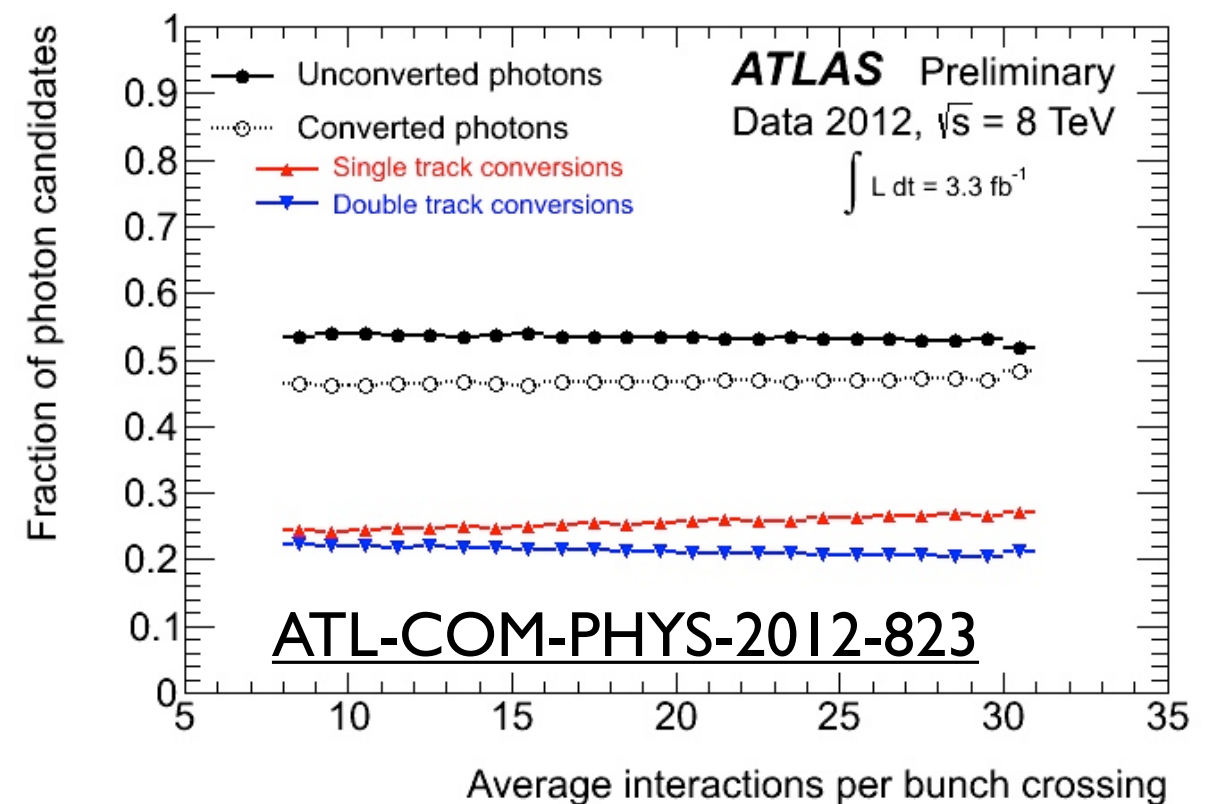
- Run 2: e/ γ reconstruction part of fully-integrated PF that follows all photon conversions and electron Bremsstrahlung
- Gaussian Sum Fitter tracking for electrons produces radiated Brem tracks
- Electron/photon candidates seeded from one of:
 - Tracker-driven GSF tracks
 - Calorimeter-driven GSF Tracks
 - EM Superclusters, assembled from PF clusters using “mustache algorithm”
- Link objects together, and attach converted tracks
- Attach clusters to tracks & Brem tangents
- Merge objects starting from different seeds
- Reject bad-quality tracks, e.g. with bad ECAL E/p or HCAL match
- Final unique event interpretation



“Mustache” clustering: allowed $\Delta\varphi$ of PF subclusters added to EM supercluster depends on $\Delta\eta$ and relative energy



- Focus of Run 2 preparation on consolidation & simplification
- Algorithm simplified
 - Uniform window size in barrel for (un)converted photons and electrons: 3x7
- Robustness against Run 2 conditions checked
 - Selection optimized, cuts tuned
 - New calibrations prepared
- Impact on conversion-finding using TRT
 - Out-of-time PU
 - Partial operation with Ar reduces PID capability (smaller effect)





- ATLAS and CMS have very different capabilities \Rightarrow different photon reconstruction strategies
 - CMS: excellent intrinsic resolution, very strong B field
 - ATLAS: multiple layers, focus on tracking (incl. PID) for conversions
- Excellent performance and successful Run I results for both detectors
- More to come in Run 2!